






Article

Potentials and Limitations of Fluviomarine Pollen Records to Reconstruct Spatiotemporal Changes in Coastal Ecosystems During the Holocene: A Case of Study from Ría de Vigo (NW Iberia)

Alberto Castro-Parada ^{1,2} , Nerea Cazás ^{1,2} , Víctor Cartelle ³ , Javier Ferreiro da Costa ⁴ ,
Natalia Martínez-Carreño ⁵, Soledad García-Gil ^{1,6}  and Castor Muñoz Sobrino ^{1,2,*} 

- ¹ Centro de Investigación Mariña, Universidad de Vigo, E-36310 Vigo, Spain; alberto.castro.parada@uvigo.gal (A.C.-P.); ncazas@alumnado.uvigo.gal (N.C.); sgil@uvigo.es (S.G.-G.)
- ² Departamento de Biología Vexetal e Ciencias do Solo, Facultade de Ciencias s/n, Universidade de Vigo, E-36310 Vigo, Spain
- ³ Flanders Marine Institute (VLIZ), InnovOcean Campus, Jacobsenstraat 1, 8400 Oostende, Belgium; victor.cartelle@vliz.be
- ⁴ GI 1934-TB (Territorio, Biodiversidade), Instituto de Biodiversidade Agraria e Desenvolvemento Rural (IBADER), Universidade de Santiago, Campus de Lugo s/n, E-27002 Lugo, Spain; javier.ferreiro@usc.gal
- ⁵ Instituto Español de Oceanografía, IEO-CSIC, C. O. Vigo, E-36390 Vigo, Spain; natalia.martinez@ieo.csic.es
- ⁶ Departamento de Xeociencias Mariñas, Facultade de Ciencias s/n, Universidade de Vigo, E-36210 Vigo, Spain
- * Correspondence: bvcastor@uvigo.es

Abstract: The study of marine and terrestrial palynomorphs in fluviomarine environments has been successfully used in combination with different geophysical approaches to understand high-resolution relative sea-level oscillations and to reconstruct the environmental changes affecting estuaries and adjacent inland ecosystems. However, erosion during the postglacial marine transgression frequently causes sedimentary discontinuities or may lead to the redeposition of ancient upland sediments, including secondary, recycled and rebedded pollen. Therefore, a robust seismic and chronological control of the sedimentary facies is essential. In addition, studies of modern pollen sedimentation and its relationship to contemporaneous vegetation are valuable for obtaining a more realistic interpretation of the sedimentary evidence. To explore the significance of the experimental evidence obtained and to support the interpretation of sedimentary records from the same basin, we analysed a large set of modern pollen data from the Ría de Vigo (NW Iberia). The pollen samples derived from different sedimentary environments were compared with the local and regional vegetation cover. Pollen evidence from the various limnetic systems studied allows the identification of major vegetation types in the basin. However, in all the cases, the reconstructed relative pollen contributions of each vegetation unit are often distorted by the overrepresentation of certain anemophilous pollen types, the underrepresentation of some entomophilous species, and the specific taphonomy of each site of sedimentation. The ability of the seabed pollen evidence to represent the modern deciduous and alluvial forests, as well as the saltmarsh vegetation onshore, increases in the shallowest points of the ria (shallower than −10 m). Conversely, pastures and crops are better represented at intermediate depths (shallower than −30 m), while scrubland vegetation is better represented in samples at more than 20 m below modern sea level. It is concluded that shallow seabed pollen can provide information on the main elements of the modern vegetation cover of the emerged basin, including the main elements of the vegetation cover. However, the selection of the most suitable subtidal sites for coring, combined with pollen data from several environmental contexts, is critical for achieving an accurate reconstruction of the changing conditions of the emerged basin over time.



Academic Editor: Shiliang Liu

Received: 29 January 2025

Revised: 24 February 2025

Accepted: 27 February 2025

Published: 5 March 2025

Citation: Castro-Parada, A.; Cazás, N.; Cartelle, V.; Ferreiro da Costa, J.; Martínez-Carreño, N.; García-Gil, S.; Muñoz Sobrino, C. Potentials and Limitations of Fluviomarine Pollen Records to Reconstruct Spatiotemporal Changes in Coastal Ecosystems During the Holocene: A Case of Study from Ría de Vigo (NW Iberia). *Land* **2025**, *14*, 540. <https://doi.org/10.3390/land14030540>

Copyright: © 2025 by the authors. Licensee MDPI, Basel, Switzerland. This article is an open access article distributed under the terms and conditions of the Creative Commons Attribution (CC BY) license (<https://creativecommons.org/licenses/by/4.0/>).

Keywords: fluvio-marine systems; pollen evidence; vegetation reconstruction; sedimentary environments; taphonomy

1. Introduction

Northwestern Iberia, located at a mid-latitude in the eastern North Atlantic margin (Figure 1), has been identified as a sensitive area to the major climatic oscillations affecting both the subtropical and the boreal North Atlantic [1–3]. Additionally, the changing marine conditions at this latitude likely contributed to governing the postglacial vegetation dynamics inland [3,4]. Over the past decades, several high-resolution pollen records were produced from aquatic systems in mountain areas and inner depressions [5–8]. Nevertheless, reconstructing the postglacial vegetation dynamics in coastal areas is challenging due to the scarcity of suitable pollen records, which are affected by both marine transgression and human modifications to the coastline. Pollen studies from the coastline are often restricted to discontinuous sequences from inactive organic deposits [9–11] or intermittently active supralittoral sedimentary systems [12–14] that can overestimate local pollen evidence [15]. To overcome these limitations, the pollen samples from shallow marine environments offer a promising alternative as they can facilitate the reconstruction of major changes affecting the coastal areas. This is particularly evident in the deepest parts of the unglaciated, partially submerged valleys (rias) [16], where deposition is almost continuous, and sedimentation rates are higher than in other parts of the basin. These environments also integrate data from both continental and marine realms [17–20]. Therefore, these complex aquatic systems present clear advantages for paleoenvironmental reconstruction in coastal areas but also pose some challenges, which can often be addressed through a multidisciplinary approach.

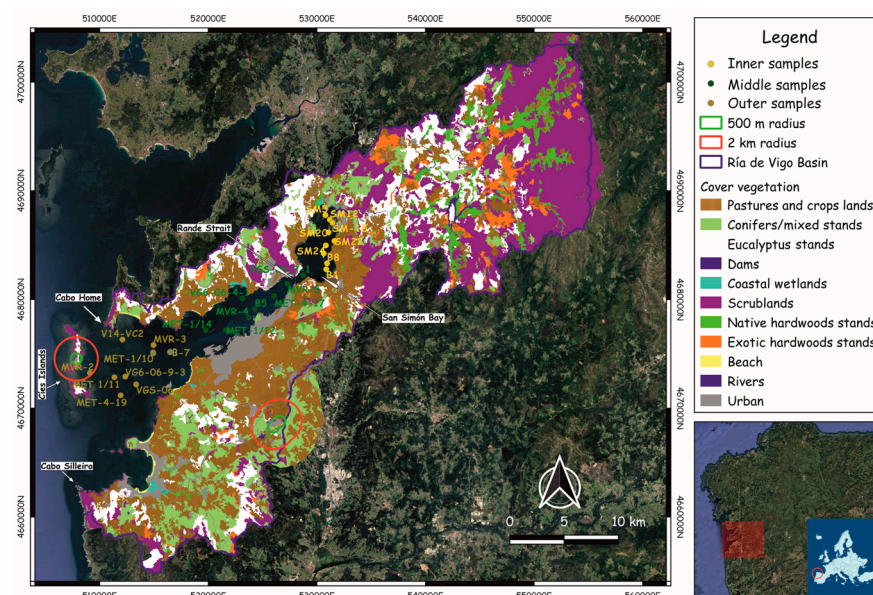


Figure 1. Location of the Galician Rías Baixas and the Ría de Vigo on the northwest coast of the Iberian Peninsula and the surface samples analysed. The extra-local (<500 m, green) and regional (<2 km, red) areas considered for the coastal lagoon and upland ponds are shown. Inner, middle, and outer seabed samples are shown in different colours. Images extracted from Google Earth Pro 7.3.6.10201.

Fluviomarine systems are key ecological zones, acting as broad ecotones between marine and upland ecosystems [21,22]. As such, they are crucial for understanding how

environmental changes, linked to both climate and human activities, impact coastal and inland ecosystems [23,24]. Marine palynomorphs from fluviomarine facies can serve as independent proxies for regional climatic inferences [25]. Furthermore, fluviomarine systems are complex sedimentary environments strongly influenced by global and relative sea-level changes [26,27]. However, spatial and temporal changes in sedimentation rates during the postglacial period result from sediment discontinuities related to marine transgression (Figure 2A), sediment reworking, biogas formation, or aquaculture practices. Other factors affecting sediment deposition in the emerged or submerged basin are shifts in weather or runoff regimes, deforestation, agricultural activity, or engineering works [20,25–29].

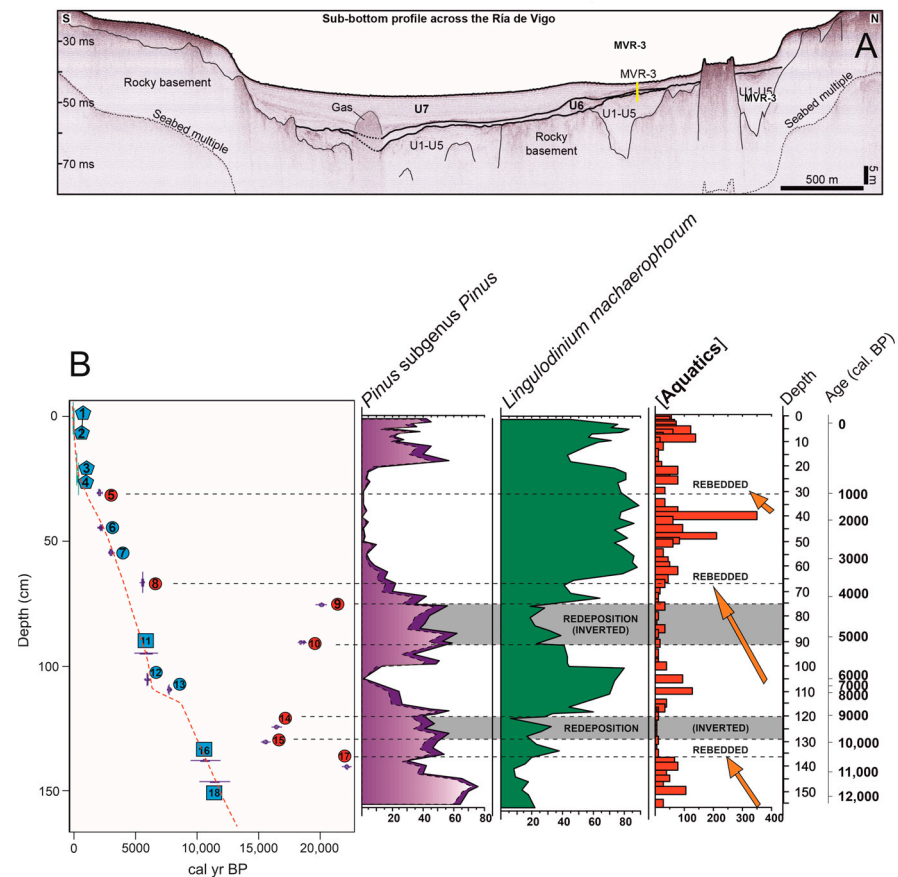


Figure 2. (A) High-resolution seismic profile (3.5 kHz) across the location of core MVR-3 and the seismic stratigraphic interpretation [25]. Seismic units are bounded by sedimentary discontinuities. U1 to U5 correspond to old Pleistocene sediments, while the Holocene is mainly represented by units U6 and U7. The thickness and distribution of each unit vary significantly along the main axis of the ria. The cloudy area (acoustic masking) in U7 denotes the presence of gas in the sediment. (B) Radiocarbon dates available and the age model produced for the core MVR-3 [25]. Dates selected for the age-depth model are highlighted in blue, and outliers in red. Pentagons indicate pollen events related to historical evidence. Squares indicate radiocarbon dates from shells, and circles represent radiocarbon dates using pollen extracted from sediment. Some outliers (e.g., 14 and 15) may be related to the accretion of upland material redeposited, inverted, in the seabed. These levels are particularly rich in *Pinus* subgenus *Pinus* (= *Diploxylon*) pollen (dark stripes). The secondary curve of percentages (dotted) represents the values recalculated after discarding the rebedded pollen underestimated. Other outliers indicate pollen material rebedded during erosive stages. The marine dinoflagellate *Lingulodinium* is independent of the redeposition of ancient upland materials but related to wet periods, as revealed by the changing Total Aquatics concentrations (grains cm⁻³) in the seabed.

Another key aspect of obtaining high-quality paleoenvironmental reconstructions is the availability of a properly defined chronological context. Biogenic carbonates are commonly used to date marine sediments via radiocarbon dating. However, radiocarbon dating in upwelling areas presents inherent calibration challenges. A correction is required to compare marine and terrestrial samples, but due to complexities in ocean circulation, the appropriate correction varies by location. Northwest Iberia, as an active upwelling area, experiences variability in upwelling intensity depending on wind strength, marine currents, and latitude [29,30], which may have fluctuated throughout the Holocene [25,31].

The regional difference from the average global marine reservoir correction is designated ΔR [32]. In the absence of a precise ΔR value for the specific region and period of interest, a suitable regional value (i.e., an appropriate but imperfect approximation) should be used. This is typically based on a series of sample pairs (marine and terrestrial) from different sites and comparable periods [33,34]. In the case of the NW Iberian Atlantic coast, the commonly used data and calculations [25,26] are provided by <http://calib.org/marine/> (accessed on 24 February 2025), which allows the selection of the 10 nearest data points available along the Atlantic coast of Iberia and employs a standardised operating method. Another limitation is that the macrofossils required for obtaining accurate dating may be sparse or irregularly present in fluviomarine sediments. This is in part due to the shallow diagenetic conditions in the Galician rias, which have resulted in widespread carbonate dissolution in recent horizons [35,36]. Additional uncertainty arises due to the marine reservoir effect, the possibility of bioturbation, and the intrusion of freshwater, which introduces older carbon (Figure 2B). Moreover, dating bulk sediment, frequently a mixture of terrestrial and marine materials in variable proportions, requires the use of mixed calibration curves. However, the reliability of some of the radiocarbon results can be compromised by the presence of gas within the sediments or the risk of carbon reservoir effect from terrestrial materials [34,36–38].

Pollen is present in many different types of sediments and ideally throughout an entire sequence. If sufficiently abundant, it can be used in radiocarbon dating when effectively isolated from other carbon-bearing materials [25,39,40]. Pollen grains are frequently abundant in estuarine and fluviomarine sediments [25,26], but maximum deposition often occurs in sedimentary environments located at some distance from the shore [41]. This is likely because the diameter (4–16 μm) and sinking rate of mineral grains closely match those of the pollen grains [42]. Furthermore, pollen is of terrestrial origin and, therefore, is not subject to the marine reservoir effect. However, dating pollen presents challenges due to differential preservation over time, which is influenced by changing taphonomic conditions [43], as well as by the intrinsic characteristics of each palynomorph. The preservation of pollen grains is directly dependent on the sporopollenin content of the grain wall [25,44,45]. Additionally, an important consideration when dating pollen is the deposition of secondary, recycled and rebedded pollen [25,46,47]. To address the challenges, combining multiple techniques, such as high-resolution seismic stratigraphy, differential radiocarbon dating, multiproxy analyses of the microscopic sediment content, or molecular studies [48], can significantly improve the interpretation of the available evidence (Figure 2B).

Nevertheless, the most important topic related to pollen evidence from fluviomarine sedimentary contexts is assessing their potential in the reconstruction of local and regional onshore changes, particularly those impacting the emerging sectors of the basin. To achieve this, pollen evidence can support reliable qualitative reconstructions and, ideally, quantitative assessments of upland vegetation [49]. Initial studies suggest that modern seabed sediments are unable to accurately capture the vegetation composition of the emerged basin [41]. For instance, *Pinus*, a bisaccate conifer pollen that is abundantly produced, relatively buoyant [50] and rich in sporopollenin [44], is frequently overrepresented in both

past [23] and modern [51–53] fluviomarine sediments. In contrast, entomophilous taxa are consistently underrepresented [20,41], although this is a common limitation in most sedimentary contexts.

In this study, we present and discuss extensive modern pollen evidence collected from different sedimentary environments within the same fluviomarine basin, the Ría de Vigo (NW Iberia). These environments include coastal lagoons, upland ponds, and subtidal seabed sediments. The pollen spectra from each sedimentary context are compared with the regional upland vegetation composition to assess the utility, advantages, and limitations of subtidal pollen evidence for palaeoenvironmental and palaeoecological studies.

2. Regional Setting

The Galician Rías Baixas, located in NW Iberia (Figure 1), consists of a coastal area characterised by an undulating relief, with medium-altitude elevations (frequently N-S oriented), alternating with small depressions. The main watersheds end in a few major, non-glaciated, flooded fluviomarine systems (rias) [16]. The bedrock is predominantly granitic, with some acid metamorphic rocks. The climate is temperate with a slight Mediterranean tendency [54], featuring an average annual temperature of 13.4 °C and total annual rainfall of 1864.3 mm [55]. This Eurosiberian territory belongs to the European Atlantic Province of the Atlantic-European Subregion [56], including the thermotemperate and mesotemperate belts. It hosts a variety of characteristic species such as *Acer pseudoplatanus* L., *Betula pubescens* Ehrh., *Daboecia cantabrica* (Huds.) K. Koch, *Frangula alnus* Mill., *Fraxinus excelsior* L., *Hypericum androsaemum* L., *Ilex aquifolium* L., *Arbutus unedo* L., *Laurus nobilis* L., *Glandora prostrata* (Loisel.) DC Thomas, *Quercus suber* L., *Quercus robur* L., *Ulex europaeus* L., *Ulex minor* Roth, and *Castanea sativa* Mill [54].

Particularly, the Ría de Vigo (Figure 1), the southernmost ria, is a drowned fluvial valley where the sea extends approximately 30 km inland from the ria's mouth to the San Simón Bay (Figure 1). Water exchange between the outer and middle parts of the ria and the San Simón Bay is limited by a narrow strait known as the Rande Strait. This shallow ria (<53 m depth) may be a key location for understanding the final stages of the marine transgression. However, the study of the shallow subsurface using seismic methods can only be conducted in some marginal areas due to the presence of shallow gas in the sediments [27]. The connection between the ria and the shelf is partially blocked by the Cíes Islands, turning the estuary into a sedimentation trap, with notable differences in grain size and sedimentation rates along its main axis [41]. Nevertheless, the available calculations for sedimentation rates are often imprecise and difficult to compare. These rates are typically derived from seismic interpretation techniques that average the physical properties, such as the estimated sound speed in different types of sediment, or from sedimentary records of varying temporal resolution obtained using different extraction methods (e.g., gravity cores, vibracores) and dating techniques (e.g., Pb isotopes, radiocarbon dating, pollen, markers) [17–20,27,35,57].

3. Materials and Methods

3.1. Pollen Samples

Lacustrine and marine deposits are important pollen reservoirs, but their pollen records can vary depending on the intrinsic characteristics of the different sedimentary environments. To determine whether the modern pollen content from sediments of coastal lagoons, upland lakes, and marine seabed deposits reflects the actual regional and extra-local vegetation composition, we analysed sixty-one modern pollen samples (Table 1) collected from the same fluviomarine basin (Ría de Vigo, NW Iberia).

In this study, we analysed the pollen content of sediments from Lagoa dos Nenos (LN), a barrier–lagoon complex in the Cíes Islands (Figure 3). It consists of a natural 1 km-long sand barrier that confines a shallow saline lagoon, whose western margin is permanently connected to the ocean, allowing water exchange during the tidal cycle (Figure 3). On the eastern side, the lagoon has another ephemeral connection to the Ría de Vigo, which is only open during winter when storm waves coincide with spring tides, causing the formation of an ephemeral inlet [14,19]. A pine plantation is located along the southern margin of the lagoon (Figures 1 and 3); the extra-local and regional vegetation include *Eucalyptus* stands, dry heaths and other plants characteristic of intertidal plains, salt marshes and meadows, salt dunes, and cliffs [19]. Pollen analysis of sediments from this open coastal lagoon (Table 1; Figure 3) aims to evaluate the influence of insularity and tidal regimes on the extra-local and regional pollen records.

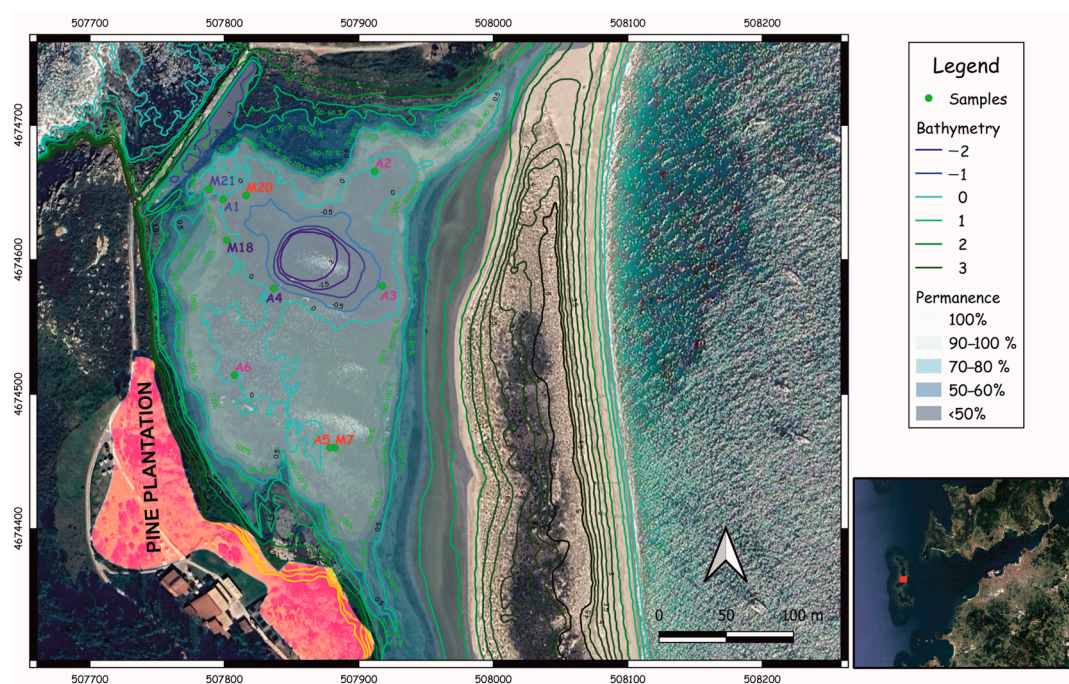


Figure 3. Lagoa dos Nenos, Cíes Islands, Ría de Vigo, showing bathymetry, tidal residence times and the pine plantation existing at its southwestern margin. The extra-local (<500 m) and regional (<2 km) vegetation composition (see Figure 1) in the islands is largely described in [19]. Images extracted from Google Earth Pro 7.3.6.10201.

Table 1. Modern samples from the Ría de Vigo basin with their altitude/depth, location in the Ría de Vigo (inner, middle or outer), groups/subgroups of samples considered for analyses, sampling year and references. For the seabed sediment samples, the water depth is expressed as m NMMA, which corresponds to the Spanish orthometric datum (mean sea level in Alicante). Positive values indicate points that emerge during low tides.

Sample	Altitude m asl/ Depth m NMMA	Environment of Sedimentation	Group of Samples	Subgroup of Samples	Subgroup of Samples	Sampling Year	References
LN/A1	0	Lagoon	Lagoon			2016	This study
LN/A2	0	Lagoon	Lagoon			2016	This study
LN/A3	−0.5	Lagoon	Lagoon			2016	This study
LN/A4	−0.5	Lagoon	Lagoon			2016	This study
LN/A5	0.5	Lagoon	Lagoon			2016	This study
LN/A6	0	Lagoon	Lagoon			2016	This study
LN/M7	0.5	Lagoon	Lagoon			2016	This study
LN/M18	0.5	Lagoon	Lagoon			2016	This study
LN/M20	−0.25	Lagoon	Lagoon			2016	This study

Table 1. Cont.

Sample	Altitude m asl/ Depth m NMMA	Environment of Sedimentation	Group of Samples	Subgroup of Samples	Subgroup of Samples	Sampling Year	References
LN/M21	0	Lagoon	Lagoon			2016	This study
P1	458	Upland Pond	Upland	Pond P		2019	49
P2	458	Upland Pond	Upland	Pond P		2019	49
P3	458	Upland Pond	Upland	Pond P		2019	49
P4	458	Upland Pond	Upland	Pond P		2019	49
P5	458	Upland Pond	Upland	Pond P		2019	49
P6	458	Upland Pond	Upland	Pond P		2019	49
L1	433	Upland Pond	Upland	Pond L		2019	49
L2	433	Upland Pond	Upland	Pond L		2019	49
L3	433	Upland Pond	Upland	Pond L		2019	49
L4	433	Upland Pond	Upland	Pond L		2019	49
L5	433	Upland Pond	Upland	Pond L		2019	49
O1	432	Drainage channel	Upland	Channel		2019	49
O2	432	Drainage channe	Upland	Channel		2019	49
O3	431	Drainage channe	Upland	Channel		2019	49
O4	431	Drainage channe	Upland	Channel		2019	49
S1	387	Upland Pond	Upland	Pond S		2019	49
S2	387	Upland Pond	Upland	Pond S		2019	49
S3	387	Upland Pond	Upland	Pond S		2019	49
S4	387	Upland Pond	Upland	Pond S		2019	49
S5	387	Upland Pond	Upland	Pond S		2019	49
S6	387	Upland Pond	Upland	Pond S		2019	49
S7	387	Upland Pond	Upland	Pond S		2019	49
S8	387	Upland Pond	Upland	Pond S		2019	49
S9	387	Upland Pond	Upland	Pond S		2019	49
S10	387	Upland Pond	Upland	Pond S		2019	49
SM12	3	Seabed sediment	Subtidal	Inner		2012	40
SM-15	3	Seabed sediment	Subtidal	Inner		2012	40
SM5	3	Seabed sediment	Subtidal	Inner		2012	40
SM20	2	Seabed sediment	Subtidal	Inner		2012	40
SM22	2	Seabed sediment	Subtidal	Inner		2012	40
SM26	−2	Seabed sediment	Subtidal	Inner		2012	40
B-8 (0-1)	−3	Seabed sediment	Subtidal	Inner		2012	40
B-1 (0-1)	−4	Seabed sediment	Subtidal	Inner		2012	40
VG6-06-4- 1 (0-2)	−13	Seabed sediment	Subtidal	Middle	Outer Rande Strait	2006	40
B-5 (0-1)	−18	Seabed sediment	Subtidal	Middle	Outer Rande Strait	2012	40
MET4/17 (0-1)	−20	Seabed sediment	Subtidal	Middle	Outer Rande Strait	2011	40
MVR-4 (0-1)	−22	Seabed sediment	Subtidal	Middle	Outer Rande Strait	2011	40
VGS- 06_7-1 (0-2)	−24	Seabed sediment	Subtidal	Middle	Outer Rande Strait	2006	40
MET-1-14 (0-2)	−26	Seabed sediment	Subtidal	Middle	Outer Rande Strait	2010	40
MET- 1/12 (0-1)	−28	Seabed sediment	Subtidal	Middle	Outer Rande Strait	2010	40
MVR-5 (0-1)	−28	Seabed sediment	Subtidal	Middle	Outer Rande Strait	2011	40
MVR-3 (0-1)	−30	Seabed sediment	Subtidal	Outer	Outer Rande Strait	2011	24
MVR-2 (0-1)	−33	Seabed sediment	Subtidal	Outer	Outer Rande Strait	2011	40
V14-VC2 (0-1)	−35	Seabed sediment	Subtidal	Outer	Outer Rande Strait	2014	40
MET- 1/11 (0-1)	−38	Seabed sediment	Subtidal	Outer	Outer Rande Strait	2010	40

Table 1. Cont.

Sample	Altitude m asl/ Depth m NMMA	Environment of Sedimentation	Group of Samples	Subgroup of Samples	Subgroup of Samples	Sampling Year	References
MET-2/10 (0-1)	−38	Seabed sediment	Subtidal	Outer	Outer Rande Strait	2010	40
VGS-06_1-1 (0-2)	−38	Seabed sediment	Subtidal	Outer	Outer Rande Strait	2006	40
VGS-06-9-3 (0-2)	−38	Seabed sediment	Subtidal	Outer	Outer Rande Strait	2006	40
MET-1-10 (0-1)	−40	Seabed sediment	Subtidal	Outer	Outer Rande Strait	2010	40
MET-4/19 (0-1)	−40	Seabed sediment	Subtidal	Outer	Outer Rande Strait	2010	40
MET-4/16 (0-1)	−42	Seabed sediment	Subtidal	Outer	Outer Rande Strait	2011	40

We included previously published modern pollen samples from the region [41,50] in our study. Pollen data from three upland ponds and the drainage channel of one of them were considered (Figure 4; Table 1). These sites are located on the main watershed at the southern margin of the Ría de Vigo. These three ponds of semi-natural origin are situated at similar altitudes (the maximum difference between them is 71 m) and within a radius of less than 1 km. However, they differ in size, the area covered by tree canopy, relative position along the main axis of the sub-basin, local vegetation and seasonality of the water table (Table 2).

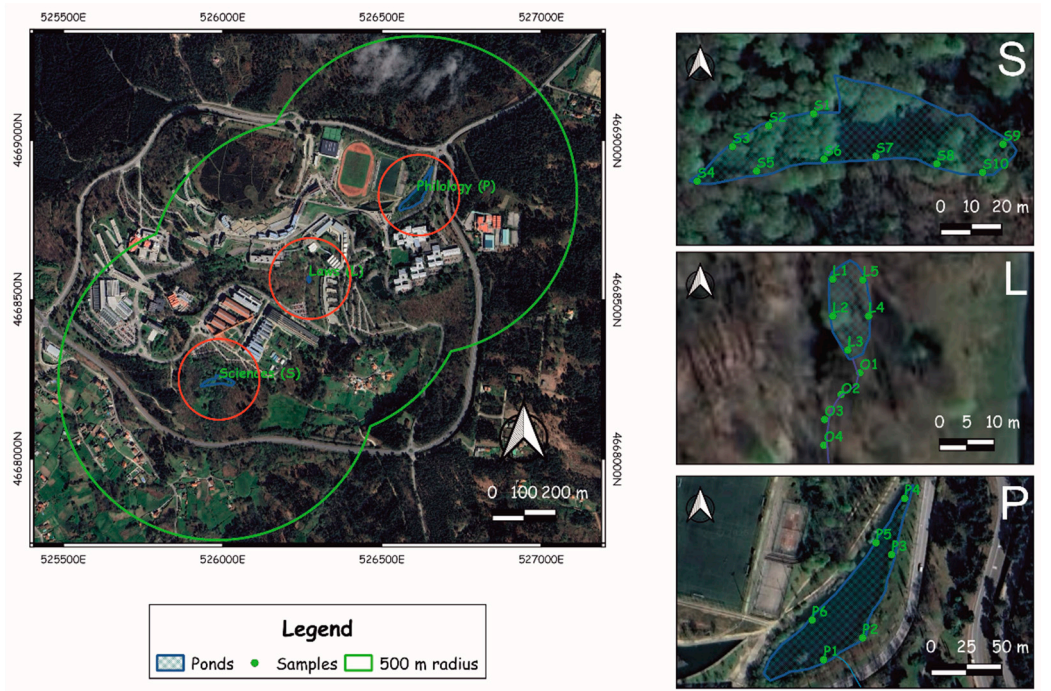


Figure 4. Detailed aerial image of the As Lagoas-Marcosende Campus, with the location of the three ponds (S, L, P) studied and the extra-local (<500 m, red) and regional (<2 km, green) areas considered. Sample locations in all the sedimentary systems analysed: Pond S, Pond L and its drainage channel (O samples), and Pond S. Table 1 indicates the main characteristics of each lacustrine system studied. Images extracted from Google Earth Pro.

Table 2. Synthesis of the main characteristics of the three upland lacustrine systems studied [50].

	Pond S	Pond L	Pond P
Surface covered by tree-canopy (%)	80	100	5
Altitude (m a.s.l.)	387	433	458
Shape	Elongated	Elliptic	Irregular
Total Surface (m ²)	2500	100	4500
Position in the sub-basin	Low	Intermediate	High
Seasonality	Marked	None	Little
Active Outflow	Winter and spring	All the year	None
Local vegetation	<i>Typha angustifolia</i> L., <i>Lemna minor</i> L., <i>Callitriche stagnalis</i> Scop., <i>Alisma plantago-aquatica</i> L., <i>Juncus effusus</i> L., <i>Iris pseudacorus</i> L., <i>Alnus glutinosa</i> (L.) Gaertn., <i>Betula pubescens</i> Ehrh., <i>Fraxinus angustifolia</i> Vahl, <i>Salix atrocinerea</i> Brot.	Bryophytes, <i>Osmunda regalis</i> L., <i>Dryopteris</i> spp., <i>Athyrium filix-femina</i> (L.) Roth, <i>Typha angustifolia</i> L., <i>Juncus effusus</i> L., <i>Potamogeton natans</i> L.	<i>Salix alba</i> L., <i>Salix atrocinerea</i> Brot., <i>Betula alba</i> L., <i>Fraxinus excelsior</i> L., <i>Alnus glutinosa</i> (L.) Gaertn., <i>Typha angustifolia</i> L., <i>Phragmites australis</i> (Cav.) Trin. Former Steud., <i>Juncus effusus</i> L., <i>Taxodium distichum</i> (L.)

We retrieved a total of 26 seabed sediment samples (Table 1) distributed across the Ría de Vigo (Figure 1). Six samples from the water-sediment interface were collected in 2012 from the shallower areas of San Simón Bay using a van Veen grab sampler. We collected additional 20 samples of surface sediment from gravity and vibracores, which were retrieved during various surveys conducted by the University of Vigo in the Ría de Vigo between 2006 and 2014. Previous studies on these samples have re-evaluated the presence of certain key palynomorphs and examined the relationships between their absolute and relative abundances and different environmental variables, including the sediment grain size, annual/seasonal precipitation, the size of the source areas, the distance to the most probable source areas, the total estimated sub-basin flow and the flowering periods [41]. The surface marine samples were divided into two main groups (Figure 1) for further analyses: 8 samples from San Simón Bay and 18 samples outside the Rande Strait. The latter group was further subdivided into two subgroups (8 from the middle ria sector and 10 from its outer part).

3.2. Chemical Treatments and Pollen Identification

All samples were dried at 80 °C for 24 h, and the dry weight and volume of each sample were measured. *Lycopodium* spores (batch 1031, Lund University, Sweden; average concentration 20,848 spores/tablet) were added to all samples to calculate pollen concentrations. The upland samples were treated with KOH [58], and the coarse fraction (>250 µm) was removed by sieving. The lagoon and seabed samples were treated with HCl and HF at room temperature to preserve the dinoflagellate cysts and foraminiferal linings content. This was followed by sieving to remove coarse (>250 µm) and fine (<10 µm) material. The 250–10 µm fraction was repeatedly washed, centrifuged (3500 rpm), and kept in a 50% glycerine–water mixture until analysis. Finally, the slides were mounted in glycerol and examined at 400× and 600× magnifications using a Nikon ECLIPSE 50i microscope

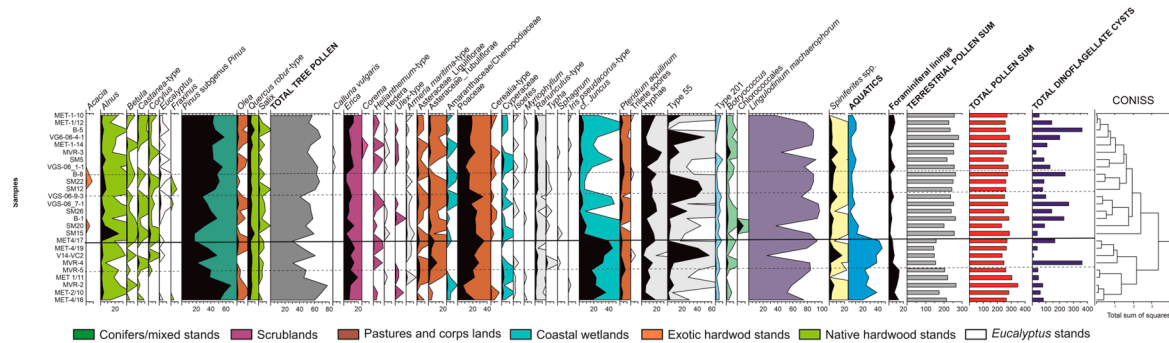


Figure 7. Summarised pollen percentages of the Ría de Vigo seabed sediment samples. The secondary pollen curves indicate $\times 10$ exaggeration. The colours indicate the vegetation units with which the pollen assemblages are associated. Horizontal line separates the two main groups of marine samples discussed in the text. Within each sample group, dotted lines separate subgroups of samples that are more similar to each other.

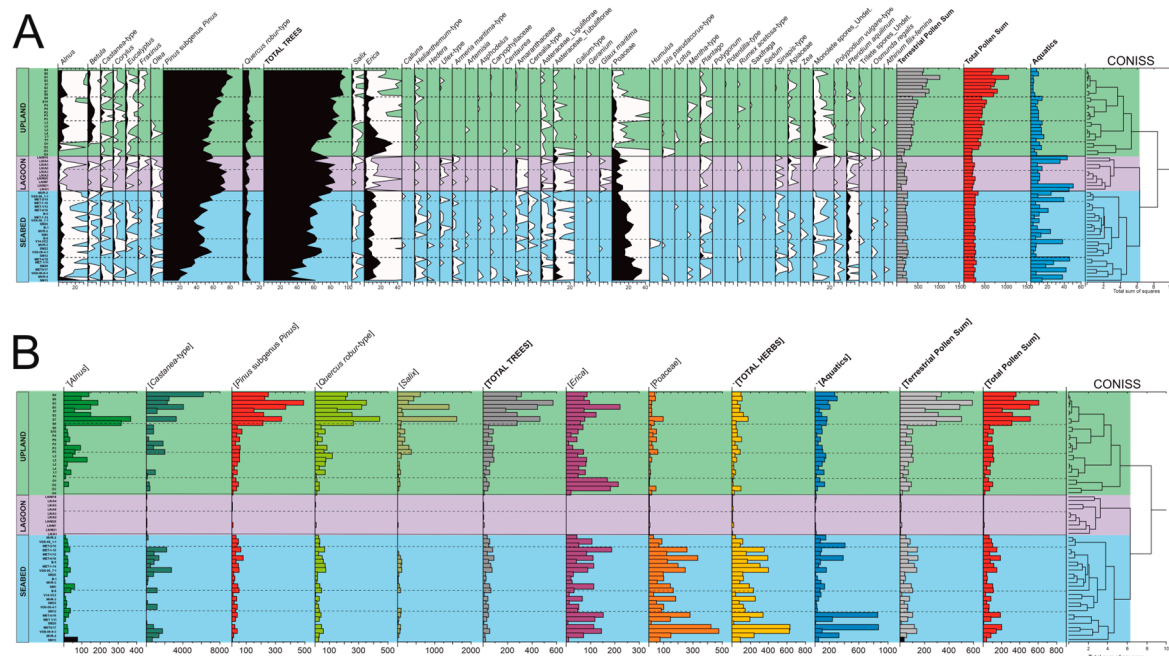


Figure 8. (A) Summarised pollen percentages and CONISS clustering for all the pollen samples analysed from the Ría de Vigo basin. (B) Pollen concentrations (grains cm^{-3}) for selected pollen types identified across all the Ría de Vigo basin samples. The coloured bars indicate upland (green), lagoon (purple) and seabed (sky blue) samples. Within each sample group, dotted lines separate subgroups of samples that are more similar to each other.

3.4. Hydrological Model of Lagoa dos Nenos

Tide and water circulation dynamics are key factors in understanding sedimentation inside the Lagoa dos Nenos (LN) coastal lagoon. To analyse these dynamics, available information relative to the local bathymetry and tidal residence times (i.e., water permanence) [64] was refined using a digital terrain model (DTM) with a 5 m resolution derived from PNOA-LIDAR data (2015–2021) [65]. These analyses were performed using the QGIS 3.40 software [66]. Georeferenced samples were processed and visualised using the same software (Figure 3).

3.5. Modern Vegetation Cover

A comprehensive study of the entire Ría de Vigo basin was also conducted using QGIS [66]. The analysis utilised a raster layer of a digital elevation model of Galicia

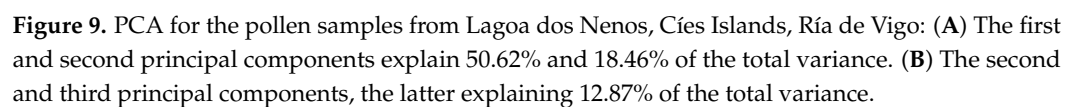
with a resolution of 25 m, incorporating contour lines and drainage basins across the whole basin area (Figure 1). The vegetation cover maps (Figure 1) were generated through photointerpretation of satellite imagery and a land-use layer [67]. The percentage of the area occupied by each vegetation unit in the whole basin was calculated using this vegetation cover and land-use map. For comparison with pollen data, vegetation units that do not produce a characteristic pollen signal (e.g., urban areas, sandy beaches, water bodies) were excluded from the analysis (Table 3). Therefore, seven main vegetation units were chosen for comparison with the modern pollen data (Figure 1): pastures and crops lands; conifers/mixed stands; *Eucalyptus* stands; coastal wetlands; scrublands; native hardwood stands; and exotic hardwood stands.

Table 3. Pollen types included in each vegetation unit discussed.

Vegetation Units	Pollen Types Included
Scrublands	<i>Calluna vulgaris</i> ; <i>Erica</i> ; <i>Corema</i> ; <i>Helianthemum</i> -type; <i>Hedera</i> ; <i>Ulex</i> -type
Pastures and crops lands	<i>Vitis</i> ; <i>Alchemilla</i> ; <i>Anchusa</i> ; <i>Armeria maritima</i> -type; <i>Artemisia</i> ; <i>Asphodelus</i> ; <i>Asteraceae_Liguliflorae</i> ; <i>Asteraceae_Tubuliflorae</i> ; <i>Brassicaceae</i> ; <i>Caryophyllaceae</i> ; <i>Centaurea scabiosa</i> ; <i>Campanula</i> -type; <i>Amaranthaceae</i> ; <i>Echium</i> ; <i>Glaux maritima</i> ; <i>Geranium</i> -type; <i>Humulus lupulus</i> -type; <i>Allium</i> -type; <i>Lotus</i> -type; <i>Mentha</i> -type; <i>Pentaglotis sempervirens</i> ; <i>Plantago</i> ; <i>Polygonum amphibium</i> ; <i>Potentilla</i> -type; <i>Rumex acetosa</i> -type; <i>Urtica</i> ; <i>Poaceae</i> ; <i>Cerealia</i> -type; <i>Zea</i> ; <i>Sedum</i> ; <i>Apiaceae</i> ; <i>Umbilicus</i> ; <i>Callitriche</i> , <i>Lythrum salicaria</i>
<i>Eucalyptus</i> stands	<i>Eucalyptus</i>
Coastal wetlands	<i>Cyperaceae</i> ; <i>Isoetes</i> ; <i>Myriophyllum</i> ; <i>Ranunculus</i> -type; <i>Typha latifolia</i> ; <i>Sphagnum</i> ; <i>Iris pseudacorus</i> -type; cf. <i>Juncus</i> ; <i>Anthoceros</i> ; cf. <i>Ruppia</i>
Conifers/mixed stands	<i>Pinus</i> subgenus <i>Pinus</i>
Exotic hardwoods stands	<i>Acacia</i>
Native hardwoods stands	<i>Alnus</i> ; <i>Betula</i> ; <i>Castanea</i> ; <i>Corylus</i> ; <i>Platanus</i> ; <i>Fraxinus</i> ; <i>Ilex</i> -type; <i>Juniperus</i> -type; <i>Arbutus</i> ; <i>Olea</i> ; <i>Populus</i> ; <i>Quercus robur</i> -type; <i>Salix</i> ; <i>Sambucus nigra</i> -type; <i>Tilia</i>

3.6. Numerical Analyses

Statistical analyses, including normality tests (Shapiro–Wilk test), Student’s *t*-test, Wilcoxon test and principal component analyses (PCA) of LN samples, were performed using PAST v.4.16c [68] and RStudio v.2022.12.10 [69]. For the PCA based on pollen percentages of modern LN samples (Figure 5), only taxa with values greater than 2% in at least two of the studied samples were considered (Figure 9). The PCA was used to identify and group the samples with similar characteristics (e.g., the role of the permanent connection to the sea, the potential sources, the transport pathways, the tidal residence times, etc.).



To evaluate the ability of pollen data to capture the vegetation diversity and composition of the whole Ría de Vigo basin (Figure 10), the different pollen types were associated with each vegetation type (Table 3), and the sums of all the percentages of the pollen types considered in each category were calculated (Figures 11–13; Table 4). For the lagoon and upland ponds, additional vegetation maps were created using a 500 m radius (extra-local) and a 2 km radius (regional) from the centre of the sedimentary systems. These maps were used to compare vegetation cover and pollen assemblages across different spatial scales (extra-local, regional and the entire basin). Marine samples were compared only with the vegetation cover of the complete basin. However, given the uneven distribution of palynomorphs along the main axis of the Ría de Vigo, as revealed by previous studies [41], several assessments were made to compare vegetation cover with different groups/subgroups of seabed pollen samples. For this, the entire Ría de Vigo dataset, the subset of samples from the middle and outer parts of the ria (outside the Rande Strait), the group of samples from the inner ria (San Simón Bay), the subgroup of samples from the middle sector of the ria, and the subset of samples from the outer ria (Figure 1; Table 1) were

considered. Average percentages were recalculated for each group/subgroup of modern samples and compared with the vegetation cover (Figures 11–13; Table 4).

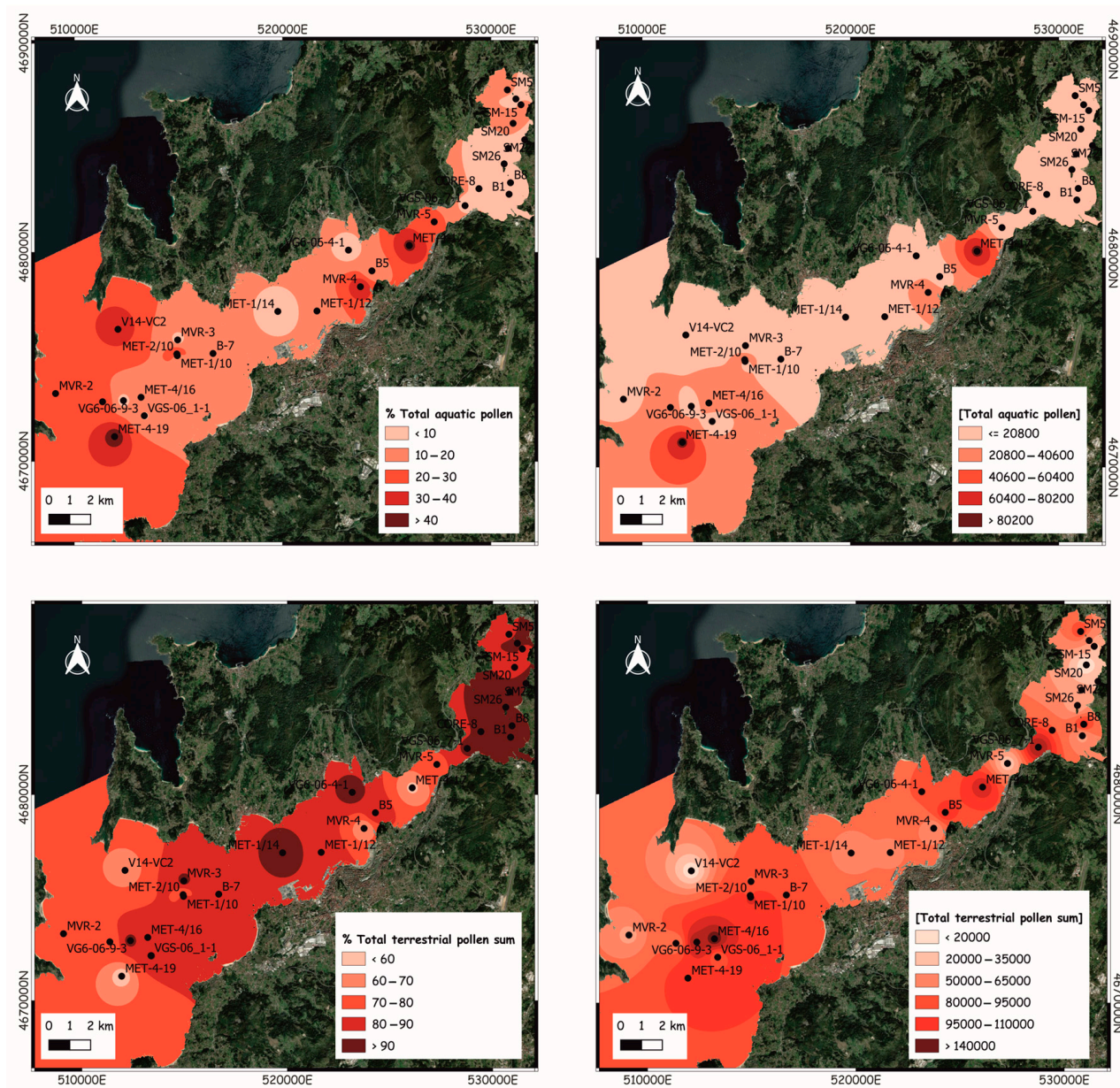


Figure 10. Percentages (left) and concentrations (right; grains/cm³) of the aquatic (above) and terrestrial (below) total pollen in modern sediments of the Ría de Vigo. Images extracted from Google Earth Pro.

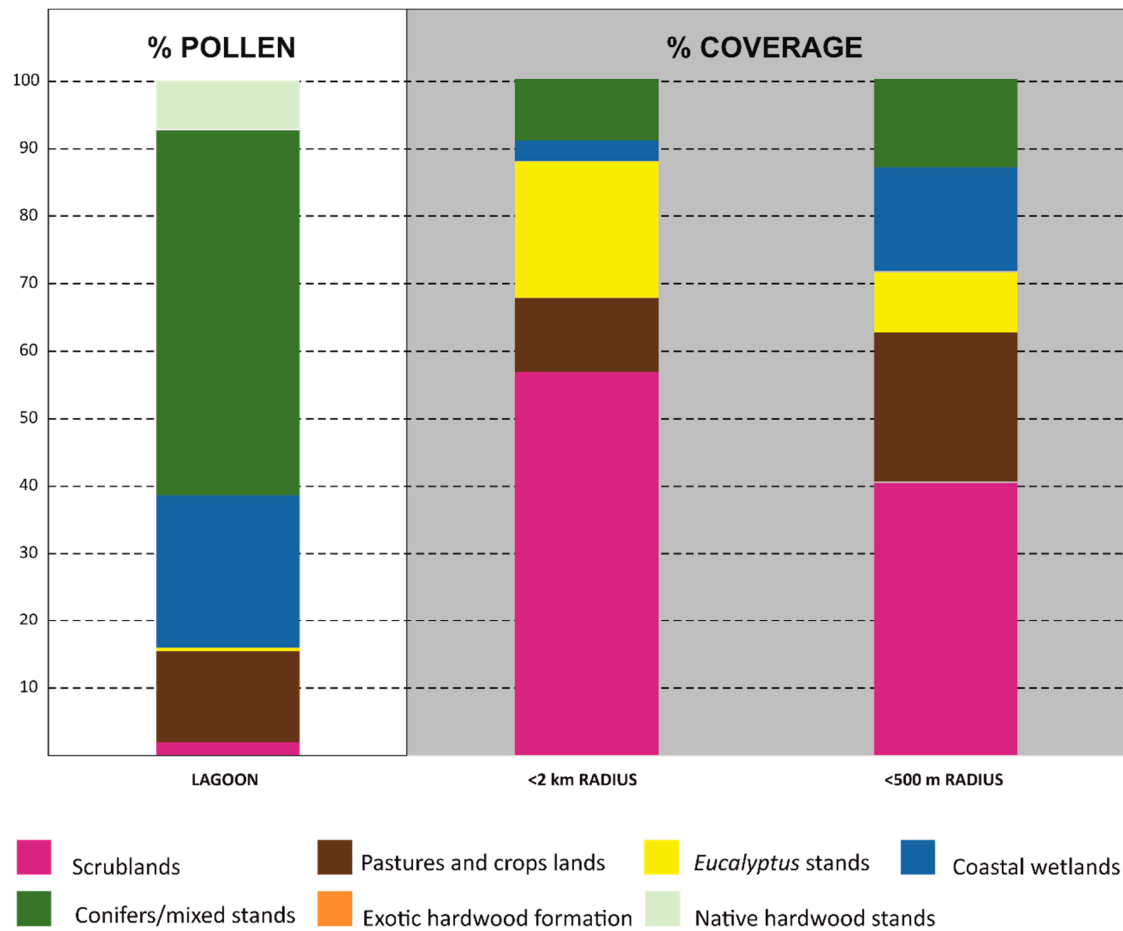


Figure 11. Average pollen samples from Lagoa dos Nenos, Cíes Islands, compared with the extra-local (<500 m) and regional (<2 km) vegetation coverage (see Figure 1 and [19]).

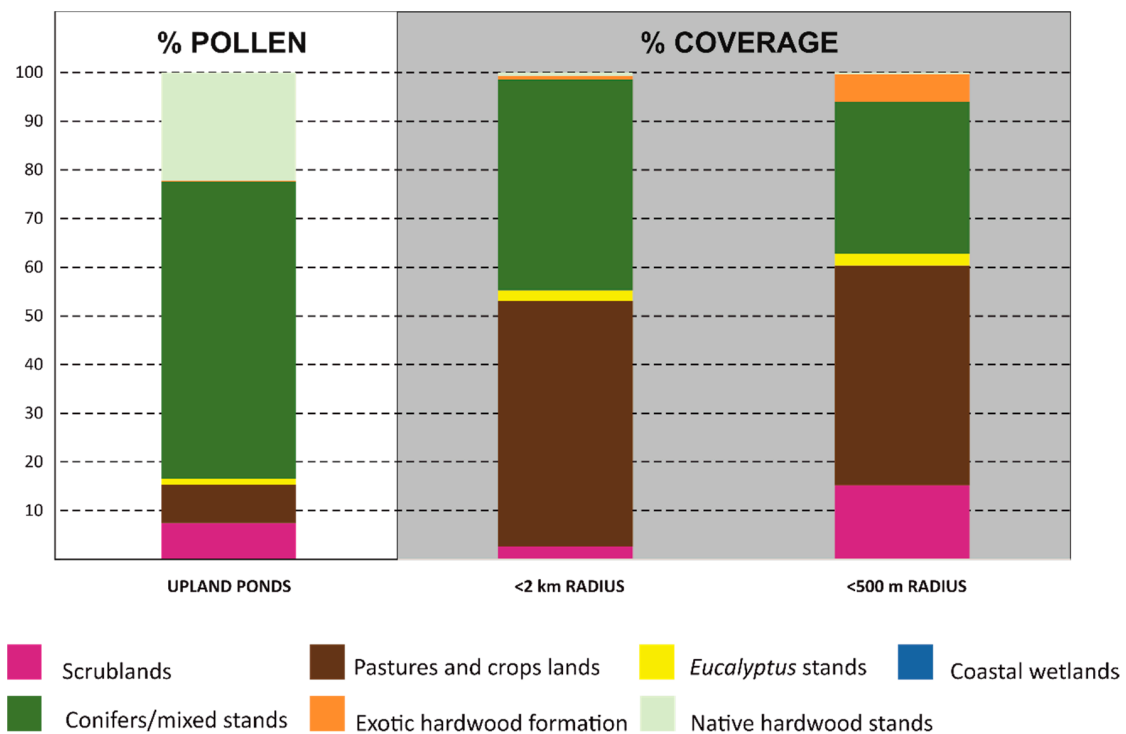


Figure 12. Average pollen samples from each upland pond analysed, averaged pollen samples for all the upland samples studied, and their comparison with the extra-local (<500 m) and regional (<2 km)

vegetation coverage (see Figures 1 and 3 and [50]) and with the vegetation cover in the Ría de Vigo basin.

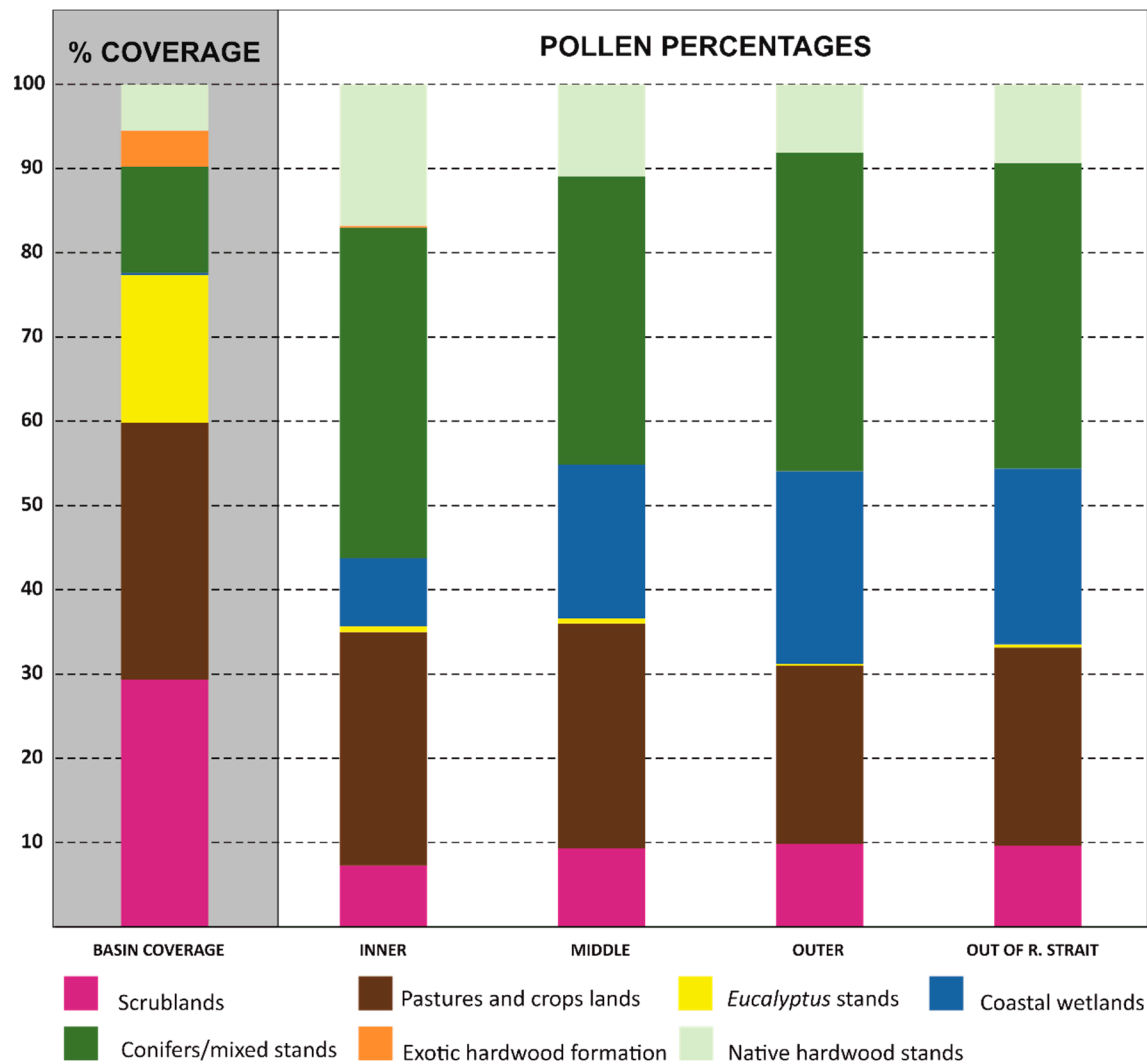


Figure 13. Average pollen samples for the complete set of subtidal samples analysed from the Ría de Vigo Ría de Vigo, the different subgroups of samples discussed (see Table 1), and their comparison with vegetation coverage within the Ría de Vigo basin (see Figure 1).

Table 4. Average pollen percentages for all the groups and subgroups of the studied samples (see Table 1) and percentages of vegetation coverages for different radii (<500 m; 2 km) and the complete Ría de Vigo (RdV) basin.

	Lagoa dos Nenos			Upland Ponds					Seabed Samples							
	Pollen	Coverage		Pollen					Coverage		Pollen					Coverage
Vegetation Units	%	< 500 m	< 2 km	% S	% L	% P	% O	% ALL	<500 m	<2 km	% All	% Inner	% Middle	% Outer	% Out R. Strait	RdV Basin
Scrublands	2.02	40.49	56.91	4.41	11.44	8.10	26.12	12.52	15.25	2.66	8.82	7.31	9.29	9.85	9.61	29.4
Pastures and crops	13.3	22.06	10.64	4.13	4.59	9.68	8.06	6.62	45.10	50.41	25.18	27.68	26.73	21.12	23.53	30.5
Eucalyptus stands	0.58	8.88	20.18	0.98	1.07	1.63	0.40	1.02	2.45	2.19	0.49	0.65	0.59	0.22	0.38	17.5
Coastal wetlands	22.79	15.43	3.10	---	---	---	---	---	---	---	16.40	8.11	18.23	22.87	20.88	0.3
Conifers/mixed stands	54.11	13.14	9.16	72.89	57.66	57.52	57.31	61.35	31.20	43.31	37.08	39.24	34.19	37.82	36.26	12.6
Native hardwood stands	7.19	---	---	17.56	25.23	23.04	8.10	18.48	0.38	0.73	11.97	16.82	10.97	8.11	9.34	5.5
Exotic hardwood stands	---	---	---	0.03	---	0.04	---	0.02	5.61	0.70	0.07	0.20	---	---	---	4.3

4. Results

4.1. Vegetation Cover in the Ría de Vigo Basin

Image analyses produced eleven coverage categories (Figure 1), but only seven may have a characteristic pollen signal (Table 3). Categories lacking a distinctive pollen signal (urban, water masses, sandy beaches) were excluded to recalculate the relative importance of each vegetation class as a percentage of the total coverage (Figures 11–13; Table 4). Scrublands, pastures and crops represent the largest coverage, each comprising about 30% of the total area. The remaining surface is covered by *Eucalyptus* stands (17.5%), conifer/mixed stands (12.6%), native hardwood stands (5.5%), exotic hardwood stands (4.3%) and coastal wetlands (0.3%).

4.2. Pollen Sedimentation in the Open Coastal Lagoon System

CONISS analysis divides the LN samples into two main groups. Group LPAZ-1 includes samples LN/A4, LN/M18, LN/A1 and LN/M21 and is characterised by higher values of cf. *Juncus* (20–40%), Poaceae (>10%) and Asteraceae Tubuliflorae (>5%) than those found in LPAZ-2 (LN/M20, LN/A5, LN/M7, LN/A3, LN/A6 and LN/A2). LPAZ-2 is characterised by a higher content of diatoms (>30%), tree pollen (*Pinus* subgenus *Pinus* > 70%; *Quercus robur*-type > 5%) and heath (*Erica*, *Corema*). Amaranthaceae are consistently present in this group (Figure 5). The total pollen concentration of the sum in the LN samples ranges from 2.2 to 13.4×10^3 grains cm^{-3} , while the terrestrial pollen concentration varies from 1.1 to 12.2×10^3 grains cm^{-3} (Figure 8B). Specifically, the *Pinus* subgenus *Pinus* pollen concentration varies considerably between the two groups of samples, averaging 3.85×10^3 grains cm^{-3} in the LPAZ-2 samples but only 1.3×10^3 grains cm^{-3} in LPAZ-1 samples.

The PCA confirms the CONISS classification of the samples (Figure 9), with the first three principal components explaining more than 80% of the total variance of the pollen diversity found in the lagoon. PC1 accounts for 50.62% of the total variance (Figure 9), and groups LN/M21, LN/A1, LN/A4 and LN/M18, which are more influenced by the tides (Figure 3) flowing through the western margin connection, positioning them on the negative side of the PC1 axis (Figure 9). In contrast, the PCA places samples LN/M7, LN/A5, LN/A3, LN/A6 and LN/A2, which are further away from the permanent connection with the open sea, into the positive part of the axis, along with sample LN/M20. This sample is relatively close to the western connection to the sea but somewhat removed from the main tidal channel (Figure 3).

In the samples located on the positive part of PC1, the pollen concentrations are higher ($>10.5 \times 10^3$ grains cm^{-3} on average; Figure 8B). The samples showing the highest pollen concentrations are dominated by *Pinus* subgenus *Pinus*, along with marine-origin elements such as central diatoms, dinoflagellate cysts, dinoflagellate vegetative cells, and, to a lesser extent, foraminiferal linings. Other pollen evidence corresponds to the regional woody vegetation (*Quercus*, *Betula*, *Olea*, *Fraxinus*, *Ulex*-type), some elements from low marshes (Amaranthaceae), sandy and wet soils (*Corema*, Apiaceae, Brassica-type, *Ranunculus*-type), and other microremains, primarily of terrestrial origin (fungal remains).

On the negative side of PC1, the pollen concentrations are lower, averaging 8.3×10^3 grains cm^{-3} (Figure 8B). The most relevant pollen elements are broadly of local origin, associated with the shallow lagoon bottom and other characteristic environments of the nearby margins, such as salt marshes and dune environments. These include Cyanobacteria, cf. *Juncus*, green algae, Asteraceae Tubuliflorae, Asteraceae Liguliflorae, and, to a lesser degree, other species linked to forest repopulations (*Eucalyptus*, *Castanea*).

PC2 accounts for 18.47% of the total variance (Figure 9). On the positive axis, it separates the samples from the deeper areas of the basin (LN/A6, LN/A4, LN/A2 and

LN/A3), i.e., those samples located in sites with high tidal residence times and water body almost permanent. The greatest weight in these samples corresponds to marine-origin elements such as dinoflagellate vegetative cells, green algae, and, to a lesser extent, central diatoms. Additionally, there is a notable presence of vegetation linked to plantations (*Eucalyptus*), crops (*Olea*) and dune systems (*Corema*, *Ulex*-type, *Apiaceae*, *Brassica*-type, *Asteraceae* Liguliflorae, *Asteraceae* Tubuliflorae). On the negative side of the axis (Figure 9), the samples are from the shallowest areas (LN/A5, LN/M7, LN/A1, LN/M20, LN/M18 and LN/M21), which are subjected to more intense tidal oscillation and longer exposure periods (Figure 3). Nonetheless, the last three samples are already close to the deeper areas and show very low (LN/M20, LN/M18) or virtually absent (LN/M21) values for this component. The most significant weight on the negative side of PC2 corresponds to pollen from anemophilous trees (*Pinus* subgenus *Pinus*, *Quercus*, *Betula*, *Fraxinus*), some elements linked to freshwater and wet soils (pennate diatoms, *Ranunculus*-type), vegetation associated with marshes and intertidal muds (Cyanobacteria, cf. *Juncus*, *Amaranthaceae*), and some marine-origin palynomorphs (dinoflagellate cysts, foraminiferal linings).

PC3 (Figure 9) accounts for 12.87% of the total variance and separates the samples LN/M18, LN/M20, LN/M7 and LN/A6 on the positive side of the axis from LN/A5, LN/A3, LA/A1, LN/M21, LN/A2 and LN/A4 on the negative side. However, the weight of this component in samples LN/M7, LN/A6 and LN/A4 is very low (Figure 9). The most significant variable on the positive side of the axis is fungal remains. Other relevant components include *Cyperaceae*, green algae, cf. *Juncus*, *Brassica*-type, and some tree elements (*Castanea*, *Eucalyptus*, *Quercus*, *Fraxinus*, *Salix*). Additionally, there are other elements with lower weights, such as microremains of marine origin (dinoflagellate cysts and foraminifera) or palynomorphs that may have been transported by marine currents penetrating the lagoon (*Erica*) [25,41].

Therefore, on the positive side of PC3, there are sampling points where the tidal flooding level fluctuates more due to the configuration of the basin, which also receives a significant lateral contribution from runoff from the surrounding land. In this group of samples (LN/M18, LN/M20, LN/M7 and LN/A6), the terrestrial/marine contribution to the sediment is more balanced. The samples with lower tidal oscillation levels (LN/A5, LN/A3, LA/A1, LN/M21, LN/A2, and LN/A4) are on the negative side of the axis. Samples LN/A5, LN/A1, and LN/M21 are in marginal areas with anoxic intertidal muds (Cyanobacteria, *Amaranthaceae*) that remain exposed for longer periods. These samples also show a higher representation of *Pinus* subsp. *Pinus* (anemophilous) and other elements linked to freshwater (*Alnus*, *Ranunculus*-type, pennate diatoms). Samples LN/A3, LNA2, and LNA4, with nearly permanent marine flooding, are rich in marine remains (dinoflagellate vegetative cells, central diatoms) but also reflect a certain contribution from the vegetation on the eastern sandy barrier (*Poaceae*, *Glaux maritima*, *Apiaceae*).

4.3. Pollen Sedimentation in the Upland Ponds

The analysis of the complete set of pollen evidence from the upland ponds reveals significant differences between the average samples from each sedimentary system and even among some samples from the same system (Figure 6). The main pollen contribution in the upland subset of samples corresponds to anemophilous species (*Pinus* subgenus *Pinus*, *Alnus*, *Betula*), which can produce large amounts of airborne pollen (Figure 6). Additionally, the fluctuating presence of *Erica* pollen cannot be directly linked to proximity to the nearest heath stands but seems to be associated with other local vegetation, such as bryophytes and ferns. This suggests that most of the heath pollen contribution comes through water flows [50]. The fact that *Erica* pollen is more efficiently transported by water flows than other pollen types [70], likely due to the better buoyancy and hydrodynamic characteristics

of its tetrads [49], supports this hypothesis. Therefore, the abundance of anemophilous pollen (which is directly related to the pond size), the tree coverage around the pond (which is inversely related to anemophilous pollen abundance), and the seasonality of the water table, which strongly determines the percentages of extra-local *Erica* and regional *Pinus* subgenus *Pinus* percentages and concentrations, are the main factors explaining these observed differences [50].

The concentration of the terrestrial pollen and the total pollen sum average 1.7×10^5 and 1.8×10^5 grains cm^{-3} , respectively (Figure 8B). However, the pollen concentration varies significantly depending on the limnetic system. Samples from stational water bodies (S1 to S8) show very high pollen accumulation, averaging 3.9×10^5 grains cm^{-3} , while those from permanently flooded ponds affected by active outflows (all P, L, and O samples, along with S9 and S10 samples) exhibit substantially lower concentrations, averaging 7.5×10^4 grains cm^{-3} [50].

4.4. Pollen Sedimentation in the Modern Subtidal Seabed

The pollen percentages identified in each surface sample from the Ría de Vigo are summarised in Figure 7. Notable pollen types identified in this complete subset of samples are *Pinus* subgenus *Pinus* (>50%) and Poaceae (20 to 40%). Additionally, the CONISS analysis separates the modern seabed samples into two groups: one with aquatic pollen largely below 20% of the total identified remains and the other with aquatic pollen ranging from 20% to more than 40% (Figure 7). Other characteristic pollen types representing deciduous trees (*Quercus robur*-type, *Betula*, *Corylus*, *Alnus*, etc.), heathlands (*Erica*), scrub (*Helianthemum*-type, *Ulex*-type), upland grassland (mainly Poaceae and Asteraceae) and marshlands (cf. *Juncus*) are consistently found across most samples, although their relative abundance varies notably between locations (Figures 7 and 10). The average total pollen concentration is 6.4×10^4 grains cm^{-3} , but it varies significantly, being relatively low ($<2 \times 10^4$ grains cm^{-3}) inside the San Simón Bay and consistently higher ($>2 \times 10^6$ grains cm^{-3}) outside of the Rande Strait (Figure 8B). This variation is primarily due to the high concentrations of both total tree pollen (almost 8×10^4 grains cm^{-3}) and total aquatic pollen ($>8 \times 10^4$ grains cm^{-3}), notably peaking in the outer part of the ria (Figure 10).

The percentages and concentrations of many palynomorphs found in seabed sediment follow a normal distribution across the Ría de Vigo. However, the abundance of several pollen types increases exponentially in certain areas, particularly *Erica*, *Alnus*, *Quercus robur*-type, *Castanea*, Poaceae and cf. *Juncus* [41]. Key factors explaining the differences in pollen representation along the main axis of the Ría de Vigo have been previously studied, concluding that the anomalous accumulation of some taxa in specific sedimentary environments may be strongly mediated by their transport via river plumes and marine currents. This includes the transport of pollen pellets as staminate catkin remains (deciduous trees), the preferential transport by flows of buoyant tetragonal tetrads (*Erica*, *Corema*), and the dragging of pollen from coastal wetlands. Many of those pollen grains are preferentially deposited when their sizes and sinking rates correspond to those of the mineral grains (silt) [41]. Furthermore, *Pinus* subgenus *Pinus* appears to be overrepresented in the average pollen signal of sediment from the Ría de Vigo seabed (Figure 7). This may be due to the high pollen productivity of pines (anemophilous species that disseminates saccate pollen through the wind), their excellent dispersal ability [42,71], and their resistance to oxidation and microbial degradation [25,44,72]. In contrast, certain pollen types are underrepresented, particularly those from exotic hardwood (mainly *Acacia*), legume and Cistaceae tickets, and *Eucalyptus*, all with predominantly entomophilous pollination syndromes [73,74].

5. Discussion

5.1. Pollen Evidence in the Ría de Vigo Basin: Differences Across Sedimentary Environments

A CONISS re-analysis for all 61 modern pollen samples, excluding those from the local vegetation components specific to each sedimentary system, confirms the grouping of samples according to their original sedimentary environments (Figure 8). The analysis consistently identifies three main clusters that separate the upland systems from the coastal lagoon and the subtidal samples (Figure 8). However, most upland samples are segregated by their respective sampling sites, with the S9 and S10 samples being notable exceptions (Figure 8). These samples, taken from the lowest points of Pond S where the water column is persistent [50], are grouped with the unseasonal, almost permanently flooded ponds P and L. Sample P1 groups more closely with the L samples than with the other P samples, due to its relatively high *Erica* values (Figure 8). The high heather pollen content likely results from a temporal stream that drains close to the P1 location (Figure 4).

The total percentages of tree pollen identified in the set of 61 modern samples fluctuate significantly, ranging from 90% to 30%, largely depending on the abundance of *Pinus* subgenus *Pinus* pollen found at each sampled station (Figure 8). *Pinus* subgenus *Pinus* is particularly abundant in sedimentary systems affected by significant water table variations, with oscillations that may be seasonal [50] (i.e., most of the markedly seasonal S samples) or influenced by the tides, as in the case of the LN samples (Figure 8). The pollen representation of deciduous oaks (*Quercus robur*-type) is relatively uniform (5–15%) across all samples, while other deciduous tree pollen, such as *Alnus* and *Betula*, show a slight increase in the upland pond samples (Figure 8). Notably, *Alnus* peaks occur in the shallowest samples of the San Simón Bay (e.g., sample SM-15; Figure 8). This has been attributed to the fluvial transport of catkins [41]. *Erica* and fern pollen values increase in subtidal sediments relative to upland pond samples but peak notably in the upland O samples from the drainage channel (Figure 7). Meanwhile, the pollen representation of upland herbs, particularly Poaceae, increases significantly in coastal and subtidal sediment samples compared with the purely terrestrial sedimentation environments (Figure 8).

The average total pollen concentration found across the different sedimentary environments in the Ría de Vigo basin exceeds 1.1×10^5 grains cm^{-3} (Figure 8B). However, it fluctuates significantly, with maximum values of more than 5×10^5 grains cm^{-3} in the more seasonally flooded samples from the lower upland Pond S [50] and minimum values of 5×10^3 grains cm^{-3} in the coastal lagoon samples (Figure 8B), where tidal movement and waves can remove part of the sedimented material (Figure 2). The fact that the lagoon is located on an island system at the mouth of the estuary and exposed to coastal winds may also negatively affect the sedimentation of extra-local anemophilous pollen (e.g., *Pinus* subgenus *Pinus*, Poaceae and others). Total pollen concentrations in the permanently flooded stations at the upland ponds average 8×10^4 grains cm^{-3} , while the average pollen concentration exceeds 6×10^4 grains cm^{-3} in the drainage channel and exceeds 9×10^4 grains cm^{-3} in the modern seabed sediments (Figure 8B). This unequal capacity for pollen accumulation may affect the ability of the sedimentary systems to accurately reflect the nearby presence of vegetation with high pollen production capacity.

5.2. Pollen Samples vs. Vegetation Types: Comparison Between Different Sedimentary Systems

To assess the ability of the different sedimentary environments to capture the extra-local, regional, and basin vegetation composition in the Ría de Vigo basin, we first examined the differences in the sum of percentages recorded in each aquatic system (Tables 3 and 5). A Student's *t*-test was used to compare the pollen percentages calculated for each vegetation category across the various groups/subgroups of samples considered with a parametric

distribution, while a Wilcoxon rank-sum test (or Mann–Whitney U test) was used for those with a non-parametric distribution (Table 5).

Table 5. Analyses of differences in pollen percentages representing each vegetation unit across the different sample groups/subgroups. Significant differences ($p < 0.05$) are shown in orange, and no significant differences ($p > 0.05$) are in white. Non-normally distributed data (tested using Shapiro–Wilk test) is presented in bold. Lack of representation shown in gray.

% Pollen	LN	Upland	P Pond	S Pond	L Pond	O Channel	All RdV	Inner	Middle	Outer	Out R. Strait	All 61 Samples
Scrublands	<0.05	<0.05	0.03	<0.05	<0.05	0.01	<0.05	<0.05	<0.05	<0.05	<0.05	<0.05
Pastures and crops	<0.05	<0.05	<0.05	<0.05	<0.05	0.125	<0.05	<0.05	<0.05	<0.05	<0.05	<0.05
Eucalyptus stands	0.02	<0.05	<0.05	<0.05	0.03	0.09	<0.05	<0.05	0.05	0.125	<0.05	<0.05
Coastal wetlands	<0.05	---	---	---	---	---	<0.05	<0.05	0.01	<0.05	<0.05	<0.05
Conifers/mixed stands	<0.05	<0.05	<0.05	<0.05	<0.05	<0.05	<0.05	<0.05	<0.05	<0.05	<0.05	<0.05
Exotic hardwood stands	<0.05	0.25	1.00	0.05	---	---	0.05	0.25	---	---	---	<0.05
Native hardwood stands	<0.05	<0.05	<0.05	<0.05	<0.05	0.01	<0.05	0.01	<0.05	<0.05	<0.05	<0.05

In the LN dataset, significant differences between samples were observed for all the vegetation units, except for the relationship between *Eucalyptus* pollen and *Eucalyptus* stands. In the upland samples, the irregular presence of *Acacia* pollen is particularly notable. *Acacia* pollen is absent from the L pond and O channel, and its percentages show no significant differences in the samples from ponds S and P (Table 5). In the P samples, no significant differences were observed for scrublands (mainly *Erica* pollen), while in the O samples, no significant differences were found for pastures and crops and *Eucalyptus* (Table 5).

Significant differences were observed across pollen percentages representing each vegetation unit for the complete Ría de Vigo subtidal dataset, except for those associated with exotic hardwood stands, primarily *Acacia* pollen (Table 5). Similar results were found (Table 5) for the inner subgroup of samples in the San Simón Bay (Table 1). Finally, for the complete set of 61 samples discussed (Table 1), significant differences were observed in the pollen percentages associated with each vegetation unit considered (Table 5).

5.3. Pollen Representation in the Coastal Lagoon vs. Vegetation Cover

The samples collected from the coastal lagoon (Figure 11; Table 4) show high pollen percentages of conifers/mixed stands (>54%), intermediate percentages of coastal wetlands (>22%), pastures and crops (>13%) and native hardwood stands (>7%). *Eucalyptus* has very low pollen representation (0.6%). Within a <500 m radius from the lagoon, vegetation cover includes 40.5% of scrublands, 22% of pastures and crops (primarily dune vegetation), 15.4% of coastal wetlands, 13% of conifers/mixed stands and ca. 9% of *Eucalyptus*. Notably, the islands lack significant native hardwood stands (Figure 1). Within a 2 km radius, the coverage percentages shift to 57% of scrublands, 20% of *Eucalyptus*, >10.5% of pastures and crops (including dune vegetation), >9% of conifers/mixed stands and 3% of coastal wetlands (Figure 11).

The pollen data reflect the nearby occurrence (<500 m) of coastal wetlands and grasslands (pastures and crops, including dune vegetation) but tend to underestimate the occurrence of *Eucalyptus* plantations and scrublands at <500 m and <2 km. Additionally, pollen data overestimate the importance of pine plantations (Figure 11; Table 4), as there is a marked overrepresentation of *Pinus* subgenus *Pinus* pollen in the lagoon compared to the surface area covered by these species both on its margins (Figure 3) and within the 2 km radius (Figure 11). Furthermore, despite the nearby presence of pine plantations, the average concentration of *Pinus* subgenus *Pinus* pollen in the lagoon samples is signif-

icantly lower than the equivalent concentrations in modern seabed samples and several orders of magnitude smaller than those found in some upland pond samples (Figure 8B). Therefore, for this coastal lagoon dataset, pollen percentages are more useful than pollen concentrations for reconstructing the extra-local vegetation of the insular system (Figure 3).

Notably, a small proportion of *Erica* pollen was found in the lagoon samples, which does not originate from the local or regional vegetation due to the absence of these species in the Cíes Islands [25]. While the shrub *Corema* (also an Ericaceae) is present in the islands, its oblate-spheroidal tetrads can generally be distinguished from the prolate-spheroidal *Erica* tetrads [75]. The nearest *Erica*-dominated shrub formations in the Ría de Vigo can be found in Cabo Home (4.3 km away) and Cabo Silleiro (12 km away, Figure 1).

5.4. Pollen Representation in Upland Ponds vs. Vegetation Cover

Previous studies conducted in these upland ponds [50] suggest that the averaged pollen records at each site reflect both the extra-local (<500 m) and the regional (<2 km) vegetation cover depending on the sedimentation systems and vegetation types (Figure 12).

For the Pond S samples, the average values align well with the extra-local and regional values for *Eucalyptus* only (Table 4) but tend to underestimate some open vegetation units (pasture and crops, scrublands) and overestimate the conifers/mixed stands. In contrast, average pollen values from Pond L overestimate scrublands and native hardwood stands while underestimating the coverage of pastures and crops and conifers/mixed stands (Table 4). Average values from Pond P samples align more closely with the extra-local vegetation cover for scrublands and conifers/mixed stands but overestimate native hardwood stands, likely due to the overrepresentation of alluvial forest pollen (Figure 12; Table 4). Finally, average values from the drainage channel (O samples) clearly overestimate the extra-local and regional importance of scrublands (Table 4).

The best fit between the vegetation categories at the extra-local and regional levels and the pollen percentages results from the averaged pollen values of the entire set of samples, regardless of the sedimentary system (Table 4). The average pollen assemblage collected from the upland sedimentary systems (Table 4; Figure 12) is dominated by pollen from conifers/mixed stands (>61%), followed by native hardwood stands (18.5%), pasture and crops (almost 7%), scrublands (12.5%), *Eucalyptus* (1%) and exotic hardwood stands (<0.05%). Consequently, this averaged pollen evidence overrepresents the regional importance of the native hardwood stands (<1%) and the presence of pine plantations within 500 m (31.2%) and 2 km (43.3%) radii while underestimating the extra-local (45.1%) and regional (50.4%) presence of pastures and crops (Table 4; Figure 12). Additionally, pollen data corresponding to scrublands almost fits (12.5%) the extra-local presence of heath (15.25%) and overrepresents its regional coverage (almost 2.7%). Exotic hardwood stands are underrepresented (5.6% at <500; 0.7% and <2 km), while *Eucalyptus* pollen data slightly underestimate its extra-local (2.4%) and regional (2.2%) coverage (Table 4; Figure 12).

5.5. Pollen Representation in Modern Seabed Sediments vs. Vegetation Cover

The full pollen dataset, consisting of 26 seabed pollen samples from the Ría de Vigo (Figure 13), reveals an over-representation of pollen associated with conifers/mixed stands (i.e., *Pinus* subgenus *Pinus*), while the pollen from exotic hardwoods stands (i.e., *Acacia*), *Eucalyptus* and scrublands (*Ulex*-type, including *Ulex*, *Cytisus* and *Genista*) are underrepresented compared to the surface area occupied by these vegetation units (Table 4; Figure 13).

The overrepresentation of *Pinus* subgenus *Pinus* may be attributed to its high pollen productivity and excellent dispersal ability. Additionally, the high sporopollenin content in the exine of *Pinus* pollen makes it resistant to oxidation and microbial degradation, enhancing its preservation in sediments. In contrast, the underrepresentation of

exotic hardwoods in the pollen record is likely due to their entomophilous pollination strategy (i.e., low pollen productivity), with pollen being dispersed as dense polyads. This also applies to *Eucalyptus* and legume thickets pollen, which share entomophilous pollination mode.

Native hardwood stands are notably overrepresented in the inner part of the ria (the San Simón Bay), but the correspondence between pollen evidence and vegetation cover is more accurate in the outer and middle parts of the ria (Figure 13; Table 4). Exotic hardwood stands have no pollen representation except for samples from San Simón Bay. Conifers/mixed stands are overrepresented in all subgroups of samples (Figure 13; Table 4), but the pollen evidence is more accurate in the middle part of the ria (Figure 13; Table 4). In contrast, the pollen representation of pastures and crops is accurate across all the sample groups, with a slight reduction in accuracy in the outer part of the ria.

Eucalyptus spp. is underrepresented in all seabed sample groups, while coastal wetlands are overrepresented in the inner, middle, and outer groups of samples, particularly in all the subsets outside of the Rande Strait (Figure 13; Table 4). The pollen representation of coastal wetlands is more accurate for the area covered by marshes within San Simón Bay (Figure 1). Finally, scrublands are underrepresented in all seabed sample groups, but their pollen representation is more accurate in the middle and outer parts of the ria (Figure 13; Table 4).

5.6. Lessons for the Interpretation of Holocene Pollen Records from Shallow Seabed Sediments

The results obtained indicate that vegetation reconstructions based on pollen content from shallow subtidal sediments are not substantially different from those derived from other upland aquatic systems. Therefore, pollen data from seabed cores recovered in incised valleys may be useful for the reconstruction of the Holocene environmental changes upland. Moreover, these sedimentary systems can capture key ephemeral ecotones, such as coastal wetlands. Variations in this type of evidence (Figure 2) may be associated with marine transgression [26,41]. Nevertheless, those sedimentary systems also have certain particularities related to the mechanisms of pollen transport, accretion, preservation and remobilisation (Figures 2 and 10) [25,41]. Previous studies in comparable fluviomarine sedimentary contexts have reported variations in the representation of different types of palynomorphs at different water depths [53,76,77]. Additionally, other studies comparing modern vegetation with pollen evidence have reported an overestimation of certain arboreal taxa and an underestimation of herbaceous elements, as well as differences across upstream-downstream gradients. The transport of pollen from the alluvial species is affected by the watershed effect [70,78]. Our results (Figures 8 and 10–13) align with many of those observations but also highlight that important differences may exist in pollen records depending on the relative position of the site studied in the submarine basin, the type of sedimentary system in which the sedimentation primarily occurred (e.g., seabed, open coastal lagoons or confined ponds) and the depositional (e.g., upwelling/downwelling regimes, rainy periods, marine currents) or post-depositional processes (e.g., upland and subtidal pollen reworked or rebedded) that influenced the sedimentation process (Figure 2).

6. Conclusions

This study analyses a comprehensive dataset of 61 pollen samples collected from various sedimentary environments within the same coastal basin of the Ría de Vigo (NW Iberia). The aquatic systems studied include an open coastal lagoon, three nearby upland ponds with differing local configurations, the drainage channel of one pond, and 26 subtidal sediment stations distributed across the inner, middle and outer sectors of the Ría de Vigo. The potential of seabed pollen in the reconstruction of upland vegetation was assessed

by comparing it to the ability of lacustrine sediments to capture the extra-local (<500 m), regional (<2 km) and complete basin vegetation composition.

Pollen evidence from all the aquatic systems investigated in this study allows the identification of the major vegetation types within the basin. However, the accuracy of reconstructed vegetation units in each case is influenced by the overrepresentation of certain anemophilous pollen types, the underrepresentation of entomophilous species and the specific taphonomy of each site.

We have found that the percentages and concentrations of the total pollen counts and most palynomorph types in the sediment of the ria follow linear growth patterns. However, several exceptions exist, notably the exponential increase in certain taxa in specific sedimentary environments (Figure 10). After comparing upland and seabed pollen evidence, we interpret this phenomenon as being strongly mediated by the transport of pollen via river plumes and marine currents [41]. The high pollen concentrations in some subtidal zones are likely driven by fluvial transport from the entire basin and specific sedimentation processes in the ria. Tidal action, which promotes the outflow of buoyant saccate pollen grains, is the main factor responsible for the significant differences in pollen concentration between the open lagoon sediment and the seabed and upland pond samples. This buoyancy phenomenon also likely drags tetrahedral *Erica* pollen into the lagoon despite the absence of this species on the Cíes Islands.

The ability of the seabed pollen evidence to represent modern deciduous and alluvial forests developed upland, as well as saltmarsh vegetation, is improved when only the pollen samples from the San Simón Bay (i.e., sites shallower than 10 m below modern sea level) are considered (Figure 1). The representation of upland pastures and croplands in the Ría de Vigo is reasonably good across the main axis of the ria pollen samples (shallower than 40 m below modern sea level), with particularly accurate pollen records in sediments from the inner and middle section of the ria (sites <30 m below modern sea level). Upland scrublands, especially heathlands, are better represented in the middle and outer parts of the ria (pollen sites deeper than 20 m below modern sea level). However, entomophilous taxa (*Eucalyptus*, *Acacia*, and legume shrubs) and anemophilous taxa (pines) stands are both underrepresented and overrepresented, respectively, in pollen samples across all the pollen stations and groups of pollen stations studied (Figure 13).

Therefore, shallow seabed pollen can provide a useful picture of the environmental conditions of the emerged basin, including the main types of vegetation cover. However, the selection of the most suitable subtidal sites for coring, combined with pollen data from several environmental contexts, is critical for achieving an accurate reconstruction of the changing conditions of the emerged basin over time. Additionally, it is important to consider that ancient upland pollen evidence may be remobilised during the marine transgression, particularly during stages of upwelling intensification, and subsequently redeposited in the seabed. To address this, differential pollen dating [25] may be necessary to assess unexpected pollen trends in the sedimentary records.

Author Contributions: Conceptualization, C.M.S.; Data curation, A.C.-P., N.C. and C.M.S.; Formal analysis, A.C.-P., N.C. and C.M.S.; Funding acquisition, S.G.-G. and C.M.S.; Investigation, C.M.S., A.C.-P. and N.C.; Methodology, V.C., N.M.-C., F.J.F.d.C. and N.C.; Project administration, C.M.S. and S.G.-G.; Software, A.C.-P., V.C. and F.J.F.d.C.; Supervision, C.M.S. and V.C.; Validation, C.M.S., S.G.-G. and A.C.-P.; Visualisation, A.C.-P. and N.C.; Writing—original draft, C.M.S.; Writing—review and editing, V.C., A.C.-P., N.M.-C., F.J.F.d.C., S.G.-G. and N.C. All authors have read and agreed to the published version of the manuscript.

Funding: This work was funded by the Spanish Ministry of Science Innovation and Universities project PID2023-147147OB-I00, financed by MICIU/AEI/10.13039/501100011033 and FEDER, UE,

and Spanish Ministry of Science and Innovation the European NextGeneration EU Funds TED2021-131141B-I00; and the Axudas Propias a Investigación da Universidade de Vigo 2024.

Data Availability Statement: The data presented in this study are available on request from the corresponding author.

Acknowledgments: The authors would like to thank I. Alejo and J.A. Fernández Bouzas for their assistance in accessing some samples and information included in this work.

Conflicts of Interest: The authors declare no conflicts of interest.

References

1. Johnsen, S.J.; Clausen, H.B.; Dansgaard, W.; Fuhrer, K.; Gundestrup, N.; Hammer, C.U.; Iversen, P.; Jouzel, J.; Stauffer, B.; Steffensen, J.P. Irregular Glacial Interstadials Recorded in a New Greenland Ice Core. *Nature* **1992**, *359*, 311–313. [\[CrossRef\]](#)
2. deMenocal, P.; Ortiz, J.; Guilderson, T.; Sarnthein, M. Coherent High- and Low-Latitude Climate Variability During the Holocene Warm Period. *Science* **2000**, *288*, 2198–2202. [\[CrossRef\]](#)
3. Muñoz Sobrino, C.; Ramil-Rego, P.; Gómez-Orellana, L.; Varela, R.A.D. Palynological Data on Major Holocene Climatic Events in NW Iberia. *Boreas* **2005**, *34*, 381–400. [\[CrossRef\]](#)
4. Roucoux, K.H.; Shackleton, N.J.; de Abreu, L.; Schönfeld, J.; Tzedakis, P.C. Combined Marine Proxy and Pollen Analyses Reveal Rapid Iberian Vegetation Response to North Atlantic Millennial-Scale Climate Oscillations. *Quat. Res.* **2001**, *56*, 128–132. [\[CrossRef\]](#)
5. Muñoz Sobrino, C.; Heiri, O.; Hazekamp, M.; Van der Velden, D.; Kirilova, E.P.; García-Moreiras, I.; Lotter, A.F. New Data on the Lateglacial Period of SW Europe: A High Resolution Multiproxy Record from Laguna de La Roya (NW Iberia). *Quat. Sci. Rev.* **2013**, *80*, 58–77. [\[CrossRef\]](#)
6. Morales-Molino, C.; García-Antón, M.; Postigo-Mijarra, J.M.; Morla, C. Holocene Vegetation, Fire and Climate Interactions on the Westernmost Fringe of the Mediterranean Basin. *Quat. Sci. Rev.* **2013**, *59*, 5–17. [\[CrossRef\]](#)
7. Iriarte-Chiapusso, M.J.; Sobrino, C.M.; Gómez-Orellana, L.; Hernández-Beloqui, B.; García-Moreiras, I.; Rodríguez, C.F.; Heiri, O.; Lotter, A.F.; Ramil-Rego, P. Reviewing the Lateglacial–Holocene Transition in NW Iberia: A Palaeoecological Approach Based on the Comparison between Dissimilar Regions. *Quat. Int.* **2016**, *403*, 211–236. [\[CrossRef\]](#)
8. van der Horst, A.; Tinner, W.; Ezquerro, F.J.; Gobet, E.; Lotter, A.F.; Morellón, M.; Sobrino, C.M.; Niffenegger, C.; Schwörer, C.; Szidat, S. Late-Glacial and Holocene Shifts in the Mountain Landscapes of the Cantabrian Range (Northern Spain) in Response to Changing Climate, Fire Occurrence and Land Use. *Quat. Sci. Rev.* **2024**, *342*, 108899. [\[CrossRef\]](#)
9. Gomez-Orellana, L.; Ramil-Rego, P.; Muñoz Sobrino, C. Una Nueva Secuencia Polínica y Cronológica Para El Depósito Pleistoceno de Mougás (NW de La Península Ibérica). *Rev. Paléobiol.* **1998**, *17*, 35–47.
10. Gómez-Orellana, L.; Ramil-Rego, P.; Muñoz Sobrino, C. The Response of Vegetation at the End of the Last Glacial Period (MIS 3 and MIS 2) in Littoral Areas of NW Iberia. *Boreas* **2013**, *42*, 729–744. [\[CrossRef\]](#)
11. Gómez-Orellana, L.; Ramil-Rego, P.; Ferreiro Da Costa, J.; Muñoz Sobrino, C. Holocene Environmental Change on the Atlantic Coast of NW Iberia as Inferred from the Ponzos Wetland Sequence. *Boreas* **2021**, *50*, 1131–1145. [\[CrossRef\]](#)
12. Santos, L.; Bao, R.; Goñi, M.S. Pollen Record of the Last 500 Years from the Doninos Coastal Lagoon (NW Iberian Peninsula): Changes in the Pollinic Catchment Size versus Paleoecological Interpretation. *J. Coast. Res.* **2001**, *17*, 705–713.
13. Danielsen, R. Palaeoecological Development of the Quiaios–Mira Dunes, Northern-Central Littoral Portugal. *Rev. Palaeobot. Palynol.* **2008**, *152*, 74–99. [\[CrossRef\]](#)
14. Costas, S.; Muñoz Sobrino, C.; Alejo, I.; Pérez-Arlucea, M. Holocene evolution of a rock-bounded barrier lagoon system, Cíes Islands, northwest Iberia. *Earth Surf. Process. Landf.* **2009**, *34*, 1575–1586. [\[CrossRef\]](#)
15. Galaz-Samaniego, C.A.; Peñalba, M.C.; Gardoki, J.; Cearreta, A.; Gómez-Arozamena, J.; Montoya-Laos, J.A.; Paz-Moreno, F.A.; Meling-López, A.E. Human-Induced Vegetation Dynamics Reconstructed through Pollen Analysis of a Recent Salt Marsh Sedimentary Sequence (Nalón Estuary, N Spain). *Wetlands* **2025**, *45*, 8. [\[CrossRef\]](#)
16. Cartelle, V.; García-Gil, S. From a River Valley to a Ria: Evolution of an Incised Valley (Ría de Ferrol, North-west Spain) since the Last Glacial Maximum. *Sedimentology* **2019**, *66*, 1930–1966. [\[CrossRef\]](#)
17. Muñoz Sobrino, C.; García-Gil, S.; Díez, J.B.; Iglesias, J. Palynological Characterization of Gassy Sediments in the Inner Part of Ría de Vigo (NW Spain). New Chronological and Environmental Data. *Geo-Mar. Lett.* **2007**, *27*, 289–302. [\[CrossRef\]](#)
18. Muñoz Sobrino, C.; García-Gil, S.; Iglesias, J.; Martínez Carreño, N.; Ferreiro Da Costa, J.; Díaz Varela, R.A.; Judd, A. Environmental Change in the Ría de Vigo, NW Iberia, since the Mid- Holocene: New Palaeoecological and Seismic Evidence. *Boreas* **2012**, *41*, 578–601. [\[CrossRef\]](#)
19. Muñoz Sobrino, C.; García-Moreiras, I.; Martínez-Carreño, N.; Cartelle, V.; Insua, T.L.; Ferreiro Da Costa, J.; Ramil-Rego, P.; Fernández Rodríguez, C.; Alejo, I.; García-Gil, S. Reconstruction of the Environmental History of a Coastal Insular System

- Using Shallow Marine Records: The Last Three Millennia of the Cíes Islands (Ría de Vigo, NW Iberia). *Boreas* **2016**, *45*, 729–753. [\[CrossRef\]](#)
20. Valero, C.; Penaud, A.; Lambert, C.; Muriel, V.; David, O.; Leroux, E.; Stéphan, P.; Siano, R.; Ehrhold, A. Holocene paleoenvironmental reconstructions in western Brittany Bay of Brest: Part I—Understanding the spatial distribution of palynological records. *Holocene* **2025**. [\[CrossRef\]](#)
 21. Traut, B.H. The Role of Coastal Ecotones: A Case Study of the Salt Marsh/Upland Transition Zone in California. *J. Ecol.* **2005**, *93*, 279–290. [\[CrossRef\]](#)
 22. Anderson, C.P.; Carter, G.A.; Waldron, M.C.B. Precise Elevation Thresholds Associated with Salt Marsh–Upland Ecotones along the Mississippi Gulf Coast. *Ann. Am. Assoc. Geogr.* **2022**, *112*, 1850–1865. [\[CrossRef\]](#)
 23. Sánchez-Goñi, M.F.; Desprat, S.; Fletcher, W.J.; Morales-Molino, C.; Naughton, F.; Oliveira, D.; Urrego, D.H.; Zorzi, C. Pollen from the Deep-Sea: A Breakthrough in the Mystery of the Ice Ages. *Front. Plant Sci.* **2018**, *9*, 38. [\[CrossRef\]](#)
 24. Ouyang, X.; Hao, X.; Culligan, N.; Dai, L.; Cheng, Z.; Li, S. Distribution of Suspended Sediments and Pollen in the Northern South China Sea: Implications for Pollen Source, Transport, and Deposition in Surface Ocean Waters. *Cont. Shelf Res.* **2021**, *231*, 104600. [\[CrossRef\]](#)
 25. Muñoz Sobrino, C.; Castro-Parada, A.; Cartelle, V.; Martínez-Carreño, N.; Delgado, C.; Cazás, N.; Lázaro, I.; García-Gil, S. Sediment Recycling during the Holocene Marine Transgression in Ría de Vigo (NW Iberia): Multiproxy Evidence and Environmental Implications. *Quat. Sci. Rev.* **2024**, *344*, 109006. [\[CrossRef\]](#)
 26. Muñoz Sobrino, C.; Cartelle, V.; Martínez-Carreño, N.; Ramil-Rego, P.; Gil, S.G. The Timing of the Postglacial Marine Transgression in the Ría de Ferrol (NW Iberia): A New Multiproxy Approach from Its Sedimentary Infill. *Catena* **2022**, *209*, 105847. [\[CrossRef\]](#)
 27. Martínez-Carreño, N.; García-Gil, S. Reinterpretation of the Quaternary Sedimentary Infill of the Ría de Vigo, NW Iberian Peninsula, as a Compound Incised Valley. *Quat. Sci. Rev.* **2017**, *173*, 124–144. [\[CrossRef\]](#)
 28. Guo, J.; Costa Jr, O.S.; Wang, Y.; Lin, W.; Wang, S.; Zhang, B.; Cui, Y.; Fu, H.; Zhang, L. Accumulation Rates and Chronologies from Depth Profiles of ²¹⁰Pb_{ex} and ¹³⁷Cs in Sediments of Northern Beibu Gulf, South China Sea. *J. Environ. Radioact.* **2020**, *213*, 106136. [\[CrossRef\]](#)
 29. Ferreira Cordeiro, N.G.; Dubert, J.; Nolasco, R.; Desmond Barton, E. Correction: Transient Response of the Northwestern Iberian Upwelling Regime. *PLoS ONE* **2018**, *13*, e0199806. [\[CrossRef\]](#)
 30. Picado, A.; Vaz, N.; Alvarez, I.; Dias, J.M. Modelling Coastal Upwelling off NW Iberian Peninsula: New Insights on the Fate of Phytoplankton Blooms. *Sci. Total Environ.* **2023**, *874*, 162416. [\[CrossRef\]](#)
 31. Martins, V.; Jouanneau, J.-M.; Weber, O.; Rocha, F. Tracing the Late Holocene Evolution of the NW Iberian Upwelling System. *Mar. Micropaleontol.* **2006**, *59*, 35–55. [\[CrossRef\]](#)
 32. Stuiver, M.; Braziunas, T.F. Modeling Atmospheric ¹⁴C Influences and ¹⁴C Ages of Marine Samples to 10,000 BC. *Radiocarbon* **1993**, *35*, 137–189. [\[CrossRef\]](#)
 33. Russell, N.; Cook, G.T.; Ascough, P.L.; Dugmore, A.J. Spatial variation in the MRE throughout the Scottish Post-Roman to late medieval period: North Sea values (500–1350 BP). *Radiocarbon* **2010**, *52*, 1166–1181. [\[CrossRef\]](#)
 34. Cook, G.T.; Ascough, P.L.; Bonsall, C.; Hamilton, W.D.; Russell, N.; Sayle, K.L.; Scott, E.M.; Bownes, J.M. Best Practice Methodology for ¹⁴C Calibration of Marine and Mixed Terrestrial/Marine Samples. *Quat. Geochronol.* **2015**, *27*, 164–171. [\[CrossRef\]](#)
 35. Álvarez-Iglesias, P.; Rubio, B.; Pérez-Arlucea, M. Reliability of Subtidal Sediments as “Geochemical Recorders” of Pollution Input: San Simón Bay (Ría de Vigo, NW Spain). *Estuar. Coast. Shelf Sci.* **2006**, *70*, 507–521. [\[CrossRef\]](#)
 36. Muñoz Sobrino, C.; Garcia-Moreiras, I.; Castro, Y.; Carreño, N.M.; de Blas, E.; Rodríguez, C.F.; Judd, A.; Garcia-Gil, S. Climate and Anthropogenic Factors Influencing an Estuarine Ecosystem from NW Iberia: New High Resolution Multiproxy Analyses from San Simón Bay (Ría de Vigo). *Quat. Sci. Rev.* **2014**, *93*, 11–33. [\[CrossRef\]](#)
 37. Kessler, J.D.; Reeburgh, W.S.; Valentine, D.L.; Kinnaman, F.S.; Peltzer, E.T.; Brewer, P.G.; Southon, J.; Tyler, S.C. A Survey of Methane Isotope Abundance (¹⁴C, ¹³C, ²H) from Five Nearshore Marine Basins That Reveals Unusual Radiocarbon Levels in Subsurface Waters. *J. Geophys. Res.* **2008**, *113*, 2008JC004822. [\[CrossRef\]](#)
 38. Alperin, M.; Hoehler, T. The Ongoing Mystery of Sea-Floor Methane. *Science* **2010**, *329*, 288–289. [\[CrossRef\]](#)
 39. Tunno, I.; Zimmerman, S.R.; Brown, T.A.; Hassel, C.A. An Improved Method for Extracting, Sorting, and AMS Dating of Pollen Concentrates from Lake Sediment. *Front. Ecol. Evol.* **2021**, *9*, 668676. [\[CrossRef\]](#)
 40. Otori, T.; Yamada, K.; Kitaba, I.; Hori, T.; Nakagawa, T. Reliable Radiocarbon Dating of Fossil Pollen Grains: It Is Truly Possible. *Quat. Geochronol.* **2023**, *77*, 101456. [\[CrossRef\]](#)
 41. Cazás, N.; Castro-Parada, A.; Cartelle, V.; Muñoz Sobrino, C. Analyses of vegetation, pollen distribution and transportation patterns in surface sediments of fluvio-marine systems (Ría de Vigo, NW Iberia): Implications for palaeoenvironmental studies. *Veg. Hist. Archaeobotany* **2025**, Submitted.
 42. Faegri, K.; Iversen, J.; Krzywinski, K. *Textbook of Pollen Analysis*, 4th ed.; John Wiley and Sons Ltd.: London, UK, 1989; p. 328.
 43. Keil, R.G.; Hu, F.S.; Tsamakis, E.C.; Hedges, J.I. Pollen in marine sediments as an indicator of oxidation of organic matter. *Nature* **2014**, *369*, 639–641. [\[CrossRef\]](#)

44. Traverse, A. *Paleopalynology*, 2nd ed.; Springer: Dordrecht, The Netherlands, 2008; p. 813. ISBN 978-1-4020-5609-3.
45. Hopkins, J.A.; McCarthy, F.M.G. Oxidation and the palynological record. *Palynology* **2002**, *26*, 266–267.
46. Li, Y.; Wang, N.; Li, Z.; Zhang, C.; Zhou, X. Reworking Effects in the Holocene Zhuye Lake Sediments: A Case Study by Pollen Concentrates AMS 14C Dating. *Sci. China Earth Sci.* **2012**, *55*, 1669–1678. [\[CrossRef\]](#)
47. Krüger, S.; Damrath, M. In Search of the Bølling-Oscillation: A New High Resolution Pollen Record from the Locus Classicus Lake Bølling, Denmark. *Veget Hist Archaeobot* **2020**, *29*, 189–211. [\[CrossRef\]](#)
48. Pawłowska, J.; Zajączkowski, M.; Łacka, M.; Lejzerowicz, F.; Esling, P.; Pawłowski, J. Palaeoceanographic Changes in Hornsund Fjord (Spitsbergen, Svalbard) over the Last Millennium: New Insights from Ancient DNA. *Clim. Past* **2016**, *12*, 1459–1472. [\[CrossRef\]](#)
49. Serge, M.-A.; Mazier, F.; Fyfe, R.; Gaillard, M.-J.; Klein, T.; Lagnoux, A.; Galop, D.; Githumbi, E.; Mindrescu, M.; Nielsen, A.B. Testing the Effect of Relative Pollen Productivity on the REVEALS Model: A Validated Reconstruction of Europe-Wide Holocene Vegetation. *Land* **2023**, *12*, 986. [\[CrossRef\]](#)
50. Castro-Parada, A.; Sobrino, C.M. Variations in Modern Pollen Distribution in Sediments from Nearby Upland Lakes: Implications for the Interpretation of Paleocological Data. *Rev. Palaeobot. Palynol.* **2022**, *306*, 104765. [\[CrossRef\]](#)
51. Dai, L.; Weng, C.; Lu, J.; Mao, L. Pollen Quantitative Distribution in Marine and Fluvial Surface Sediments from the Northern South China Sea: New Insights into Pollen Transportation and Deposition Mechanisms. *Quat. Int.* **2014**, *325*, 136–149. [\[CrossRef\]](#)
52. Luo, C.; Chen, M.; Xiang, R.; Liu, J.; Zhang, L.; Lu, J.; Yang, M. Modern Pollen Distribution in Marine Sediments from the Northern Part of the South China Sea. *Mar. Micropaleontol.* **2014**, *108*, 41–56. [\[CrossRef\]](#)
53. Yedema, Y.W.; Donders, T.; Peterse, F.; Sangiorgi, F. Dinoflagellate Cyst and Pollen Assemblages as Tracers for Marine Productivity and River Input in the Northern Gulf of Mexico. *J. Micropalaeontol.* **2023**, *42*, 257–276. [\[CrossRef\]](#)
54. Rodríguez Guitián, M.; Ramil-Rego, P. Fitogeografía de Galicia (NW Ibérico): Análisis Histórico y Nueva Propuesta Corológica. *Recur. Rurais* **2008**, *4*, 19–50. [\[CrossRef\]](#)
55. Meteogalicia. Unidade de Observación e Predicción Meteorolóxica. 2021. Available online: <https://www.meteogalicia.gal/observacion/estacionshistorico/historico.action?idEst=10161> (accessed on 9 January 2025).
56. Rodríguez Guitián, M.; Ramil-Rego, P. Clasificaciones Climáticas Aplicadas a Galicia: Revisión Desde Una Perspectiva Biogeográfica. *Recur. Rurais* **2007**, *3*, 31–53. [\[CrossRef\]](#)
57. García-Moreiras, I.; Pospelova, V.; García-Gil, S.; Sobrino, C.M. Climatic and Anthropogenic Impacts on the Ría de Vigo (NW Iberia) over the Last Two Centuries: A High-Resolution Dinoflagellate Cyst Sedimentary Record. *Palaeogeogr. Palaeoclimatol. Palaeoecol.* **2018**, *504*, 201–218. [\[CrossRef\]](#)
58. Moore, P.D.; Webb, J.A.; Collinson, M.E. *Pollen Analysis*, 2nd ed.; Blackwell Scientific Publications: Oxford, UK, 1991.
59. Valdés, B.; Díez, M.J.; Fernandez, I. *Atlas Polínico de Andalucía Occidental*; Instituto de Desarrollo Regional de la Universidad de Sevilla, Excma; Diputación de Cádiz: Sevilla, España, 1987.
60. Reille, M. *Pollen et Spores d'Europe et d'Afrique du Nord, Supplément 1*, 1st ed.; Laboratoire de Botanique Historique et Palynologie: Marseille, France, 1995.
61. Reille, M. *Pollen et Spores d'Europe et d'Afrique du Nord, Supplément*, 2nd ed.; Laboratoire de Botanique Historique et Palynologie: Marseille, France, 1998.
62. Reille, M. *Pollen et Spores d'Europe et d'Afrique du Nord*, 2nd ed.; Laboratoire de Botanique Historique et Palynologie: Marseille, France, 1999.
63. Grimm, E. TILIA and TILIA graph: PC spreadsheets and graphics software for pollen data. *INQUA Comm. Study Holocene Work. Group Data Handl. Methods Newsl.* **1990**, *4*, 5–7.
64. López, F.; Vigo, M.A. *Estudio Básico. Gestión de la Laguna Costera “Lago dos Nenos” en el Archipiélago de Cíes*; Xunta de Galicia: Vigo, Pontevedra, 2016.
65. PNOA-LIDAR. Plan Nacional de Ortofotografía Aérea. Plan Nacional de Observación del Territorio. Instituto Geográfico Nacional 2015–2021. Available online: <https://pnoa.ign.es/web/portal/pnoa-lidar/estado-del-proyecto> (accessed on 14 February 2025).
66. QGIS.org. QGIS 3.40.2 ‘Bratislava’. GIS Geographic Information System. QGIS Association 2024. Available online: <http://www.qgis.org> (accessed on 25 November 2024).
67. IET. Mapas de Usos e Coberturas do Solo 2017. Available online: <http://descargas.xunta.es/fb5738cd-788f-4b8d-ac66-96abbaccde1495189290462> (accessed on 7 December 2021).
68. Hammer, O.C.; Harper, D.A.T.; Ryan, P.D. PAST: Paleontological Statistics software package for education and data analysis. *Palaeontol. Electron.* **2001**, *4*, 9.
69. R Core Team. R: A Language and Environment for Statistical Computing. R Foundation for Statistical Computing 2021, Vienna, Austria. Available online: <https://www.R-project.org/> (accessed on 10 December 2024).
70. Brown, A.G.; Carpenter, R.G.; Walling, D.E. Monitoring Fluvial Pollen Transport, Its Relationship to Catchment Vegetation and Implications for Palaeoenvironmental Studies. *Rev. Palaeobot. Palynol.* **2007**, *147*, 60–76. [\[CrossRef\]](#)

71. Quamar, M.F.; Mishra, A.K.; Mohanty, R.B.; Kar, R. Implications of *Pinus* L. Pollen Abundance for Reconstructing the Holocene Palaeoclimate from the Himalayas, India. *Rev. Palaeobot. Palynol.* **2024**, *326*, 105130. [[CrossRef](#)]
72. Havinga, A.J. A 20-Year Experimental Investigation into the Differential Corrosion Susceptibility of Pollen and Spores in Various Soil Types. *Pollen Spores* **1984**, *26*, 541–557.
73. Rodríguez-Rajo, F.J.; Jato, M.V.; Seijo, M.C. El Polen de *Eucalyptus* y su incidencia en la atmósfera de Vigo (NO España). *Acta Botánica Malacit.* **2001**, *26*, 99–110. [[CrossRef](#)]
74. Ollerton, J.; Alarcón, R.; Waser, N.M.; Price, M.V.; Watts, S.; Cranmer, L.; Hingston, A.; Peter, C.I.; Rotenberry, J. A Global Test of the Pollination Syndrome Hypothesis. *Ann. Bot.* **2009**, *103*, 1471–1480. [[CrossRef](#)] [[PubMed](#)]
75. Nunes Morgado, L.; Gonçalves-Esteves, V.; Resendes, R.; Mateus Ventura, M.A. A pollen inventory of endemic species from the Azores archipelago, Portugal. *Palynology* **2018**, *42*, 273–289. [[CrossRef](#)]
76. Solomon, S.; Mudie, P.J.; Cranston, R.; Hamilton, T.; Thibaudeau, S.A.; Collins, E.S. Characterisation of marine and lacustrine sediments in a drowned thermokarst embayment, Richards Island, Beaufort Sea, Canada. *Int. Journal Earth Sci.* **2000**, *89*, 503–521. [[CrossRef](#)]
77. Mudie, P.J.; Yanko-Hombach, V.V.; Mudryk, I. Palynomorphs in surface sediments of the North-Western Black Sea as indicators of environmental conditions. *Quat. Int.* **2021**, *590*, 122–145. [[CrossRef](#)]
78. Lambert, C.; Vidal, M.; Penaud, A.; Combourieu-Nebout, N.; Lebreton, V.; Ragueneau, O.; Gregoire, G. Modern palynological record in the Bay of Brest (NW France): Signal calibration for palaeo-reconstructions. *Rev. Palaeobot. Palynol.* **2017**, *244*, 13–25. [[CrossRef](#)]

Disclaimer/Publisher’s Note: The statements, opinions and data contained in all publications are solely those of the individual author(s) and contributor(s) and not of MDPI and/or the editor(s). MDPI and/or the editor(s) disclaim responsibility for any injury to people or property resulting from any ideas, methods, instructions or products referred to in the content.